Sex-specific Acute Cerebrovascular Response to Photothrombotic Stroke in Mice Requires Rho-kinase

Joanna Raman-Nair

Thesis submitted to the University of Ottawa

in partial fulfillment of the requirements for

the Master of Science degree in Neuroscience

Department of Cellular and Molecular Medicine

Faculty of Medicine

University of Ottawa

Abstract

With high energy consumption and a low capacity for energy storage, the brain is highly dependent on a continuous supply of oxygen and nutrients from the bloodstream. Ischemic stroke, caused by the occlusion of a cerebral blood vessel, compromises cerebral blood flow (CBF), resulting in detrimental effects on brain homeostasis, vascular function, and neuronal health. Sex differences in ischemic stroke are known, with women having lower rates of stroke due to a protective role of estrogens on vascular health, and more severe strokes following reduced estrogen production after menopause. Rho-associated protein kinase (ROCK), an important regulator of vascular tone, also regulates vascular function in a sex-specific manner, and its deletion is neuroprotective following ischemic stroke. The current study explores the overlapping roles of ROCK and endogenous hormone influence on the acute CBF response to a photothrombotic (PT) model of ischemic stroke in mice. CBF was measured following stroke in the somatosensory cortex in mice with a heterozygous deletion of the ROCK2 isoform (*ROCK2*$^{+/-}$) and in wild-type (WT) littermates. To remove endogenous hormones, male mice were gonadectomized (Gdx) and female mice were ovariectomized (Ovx), and control animals received a sham surgery ("intact") prior to stroke induction. Intact WT males showed a delayed CBF drop compared to intact WT females, where peak drop in CBF wasn't observed until 48 hours following stroke. Gonadectomy in males did not alter this response, however ovariectomy in females produced a "male-like" response. *ROCK2*$^{+/-}$ males also showed such phenotypic response, and Gdx did not alter this response, suggesting ROCK2 deletion or endogenous male hormones do not alter CBF response in males in this stroke model. Alternatively, intact *ROCK2*$^{+/-}$ females showed a striking difference in CBF values compared to intact WT females, where they displayed higher CBF values immediately post-stroke and also showed a peak drop in CBF at 48 hours post-stroke. Ovx did not change the CBF response in *ROCK2*$^{+/-}$ females. Overall, there is a marked difference between males and females in their acute CBF responses to PT stroke, which appears to be mediated by endogenous female sex hormones and ROCK2. All groups except for intact WT females show a delayed drop in CBF values, reaching a maximal drop in CBF at 48 hours following stroke induction. This may be due to hyperreactivity of female platelets and upregulation of RhoA/ROCK signaling in female platelets. Further research is required to confirm this speculation. This study reveals important sex-differences and the involvement of ROCK2 in acute CBF responses to PT stroke in mice.

Table of Contents

Acknowledgements

First and foremost, I would like to sincerely thank my supervisor, Dr. Baptiste Lacoste, for his endless dedication and guidance throughout my master's. Without his expertise and knowledge, this project would not have been possible. He allowed me the space and time to grow into the scientist I am today, and for that I am eternally grateful.

I would like to extend this appreciation to fellow lab members, past and present, of the Lacoste lab. Whether it was to trouble shoot an experiment, help out with lab work, or just general comradery, their presence facilitated my time at the lab and made the experience enjoyable. With my colleagues' support and advice, I have learned many new skills and created memories I will cherish forever.

This project would not have been possible without all the people that helped along the way. I would like to thank the University of Ottawa's Animal Care and Veterinary Services for providing training, equipment, and expertise for all *in vivo* experiments performed. I would also like to express my sincere gratitude to the University of Ottawa's Preclinical Imaging Core facility and Dr. Gregory Cron, who performed all MRI scanning and was an integral part in facilitating my data collection. Additionally, I would like to express my appreciation for Dr. Dale Corbett and Dr. Jean-Claude Béïque, whom both served as members of my Thesis Advisory Committee and challenged my perspectives to become a better scientist. Finally, many thanks to Dr. Kathleen MacLeod from the University of British Colombia who provided our lab with the *ROCK2*$^{+/-}$ mice used in this study.

Lastly, I would like to thank my family and friends for their words of encouragement throughout the course of my master's, especially in the last few months as this project has wrapped up. Their support helped me stay on track and complete this achievement.

Appendix

The following papers were published during the completion of my masters. Not all pertain to the subject of this thesis.

Martin, M., Bostaille, N., Eubelen, M., Spitzer, D., Profaci, C. P., Toussay, X., **Raman-Nair, J**., Pozuelo, E., Vermeiren, S., Tebabi, P., America, M., Sandersson, L., Cabochette, P., Germano, R. F. V., Torres, D., Boutry, S., de Kerckhove, A., Bellefroid, E., Devraj, K., Lacoste, B., Daneman, R., Liebner, S. & Vanhollebeke, B. (2022). Engineered Wnt ligands enable blood-brain barrier repair in neurological disorders. *Science*, 375(*6582*): eabm4459. https://pubmed.ncbi.nlm.nih.gov/35175798/

Bordeleau, M., Comin, C. H., Fernández de Cossío, L., Lacabanne, C., Freitas-Andrade, M., González-Ibáñez, F., **Raman-Nair, J.**, Wakem, M., Chakravarty, M., da F. Costa, L., Lacoste, B., & Tremblay, M.-E. (2022). Maternal high-fat diet in mice induces cerebrovascular, microglial and long-term behavioural alterations in offspring. *Communications Biology*, 5(*1*): 26. https://pubmed.ncbi.nlm.nih.gov/35017640/

Freitas-Andrade, M., **Raman-Nair, J.**, & Lacoste, B. (2020). Structural and functional remodeling of the brain vasculature following stroke. *Frontiers in Physiology*, 11: 1-28. https://pubmed.ncbi.nlm.nih.gov/32848875/

List of Figures

List of Abbreviations

BBB – blood-brain barrier

CBF – cerebral blood flow

DHT – dihydrotestosterone

E2 – 17β-estradiol

ECs – endothelial cells

eNOS – endothelial nitric oxide synthase

ERs – estrogen receptors

ERα – estrogen receptor-α

ERE – estrogen response elements

ET-1 – endothelin-1

GC – guanylyl cyclase

Gdx – gonadectomy

HIF-1α – hypoxia-inducible factor 1α

K/X – ketamine/xylazine

LDF – laser doppler flowmetry

MCAo – middle cerebral artery occlusion

MLC – myosin light chain

MLCP – myosin light chain phosphatase

MRI – magnetic resonance imaging

NO – nitric oxide

NVC – neurovascular coupling

NVU – neurovascular unit

Ovx – ovariectomy

PBS – phosphate buffered saline

PI3K – phosphatidylinositol-3-kinase

PT – photothrombotic

RB – rose bengal

ROCK – Rho-associated coiled-coil containing protein kinase

ROI – region of interest

ROS – reactive oxygen species

rtPA – recombinant tissue plasminogen activator

SC – subcutaneous

VEGF – vascular endothelial growth factor

VSMCs – vascular smooth muscle cells

WT – wild-type

1. Introduction

1.1 Regulation of Blood Flow in the Healthy Brain

While the brain only accounts for 2% of a person's body mass, it requires a substantially greater proportion of energy to maintain normal function. Approximately 20% of cardiac output is directed to the brain to ensure metabolic needs of the brain are met, thus healthy vasculature is essential to preserve neuronal health (Andreone, et al., 2015; Attwell & Laughlin, 2001; Peters, et al., 2004). Brain function is therefore reliant on key vascular features: *i)* the maintenance of vascular networks for efficient perfusion, *ii)* the function of the blood-brain barrier (BBB) to preserve brain homeostasis, and *iii)* the regulation of cerebral blood flow (CBF) to match neuronal demands (Andreone, et al., 2015; Lacoste & Gu, 2015). With high energy consumption and a low capacity for energy storage, the brain is highly dependent on a continuous supply of oxygen and nutrients from the bloodstream. To accommodate high metabolic demands, cerebral blood vessels have an inherent capability to modulate perfusion such that the brain receives blood flow at a continuous rate despite changing values of blood pressure in the periphery, a phenomenon termed cerebral autoregulation. This is achieved by modifying cerebral vascular resistance mainly in pial and parenchymal arteries (Moshayedi & Liebeskind, 2021).

A dynamic relationship between neural and vascular cells facilitates neurovascular coupling (NVC), another mechanism by which the brain ensures stable perfusion via a functional matching between metabolic demand and perfusion such that increased neuronal activity leads to increased CBF (Hillman, 2014). This response is made possible by the intimate anatomical relationship between neuronal, glial, and vascular systems (Lecrux & Hamel, 2011). The anatomical substrate of NVC is the neurovascular unit (NVU), a multicellular complex in which pericytes, astrocytes, microglia, neurons, and endothelial cells (ECs) orchestrate brain and

vascular function (**Fig. 1**) (Cauli & Hamel, 2010; Attwell, et al., 2010; Howarth, 2014). Neurons and glia facilitate NVC via balanced secretions of vasoactive molecules targeted at dilating or constricting surrounding vessels to regulate CBF (Attwell, et al., 2010; Cauli & Hamel, 2010; Mishra, et al., 2016; Girouard & Iadecola, 2006). Cells of the NVU also maintain the integrity of the BBB, which controls the passage of substances into the brain, establishing a controlled homeostasis (Daneman, 2012; Profaci, et al., 2020). Structural and functional interdependence between brain cells and blood vessels, coordinated by cellular and molecular crosstalk, renders the brain particularly vulnerable to declines in CBF that result from stroke.

ECs are master regulators of CBF and NVC in the healthy brain, particularly through the production of vasodilatory nitric oxide (NO) via the enzyme endothelial nitric oxide synthase (eNOS) (Yamada, et al., 2000). Activation of eNOS is triggered by direct phosphorylation, high fluid shear stress on ECs, increases in intracellular Ca^{2+} concentration, or through the binding of several agonists, including acetylcholine (Fleming, 2010). NO produced in ECs quickly diffuses into nearby vascular smooth muscle cells (VSMCs), regulating vascular tone via activation of soluble guanylyl cyclase (GC) and subsequent cyclic guanosine monophosphate (cGMP) production (Zhao, et al., 2015). Even partial modulation of eNOS is sufficient to induce large changes in CBF (Samdani, et al., 1997). Under pathological conditions, dysregulation of eNOS activity has been demonstrated in cardiovascular disease, vascular aging, vascular dementia and stroke (Sawada & Liao, 2009; Toda, et al., 2009; Toda, 2012; Zhu, et al., 2016; Wang, et al., 2018). Another regulator of vascular tone, endothelin-1 (ET-1), is a potent vasoconstrictor produced in ECs mainly due to hypoxia and low shear stress (Kowalczyk, et al., 2015). Under physiological conditions, NO and ET-1 originating from ECs are in a constant dynamic balance with other vasoactive molecules to regulate vascular tone.

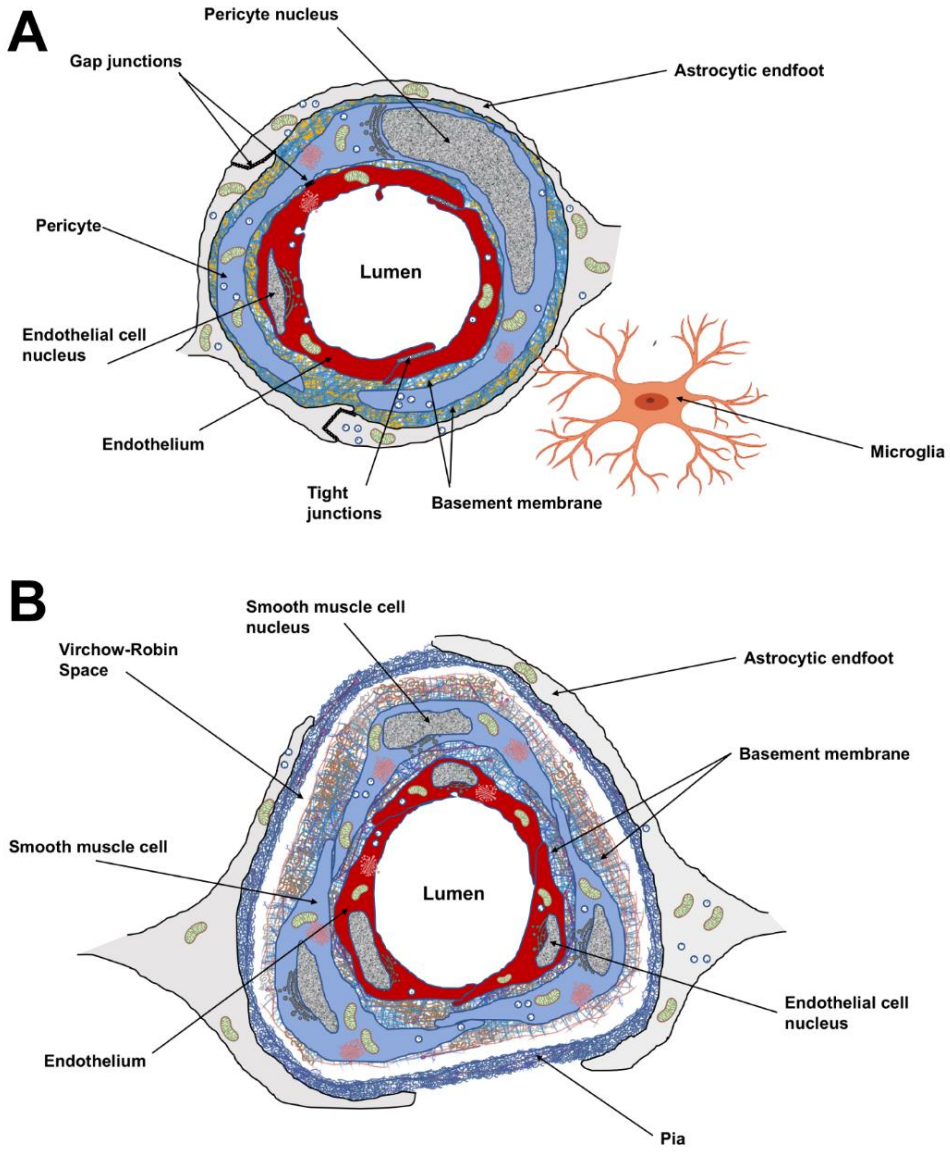

Figure 1. Cellular and acellular constituents of the neurovascular unit (NVU).

(**A**) At the level of the intracerebral capillaries, the NVU is comprised of endothelial cells, pericytes, astrocytes, microglia and the basement membrane. Both the endothelial cells and surrounding pericytes are unsheathed by a common basement membrane. The pericyte processes encase most of the endothelial surface. Astrocyte endfeet completely surround the capillary wall. Resting microglial have a ramified morphology and are in constant surveillance around brain microvessels. Gap junction channels enable cytoplasmic continuity between astrocytic endfeet. Gap junction channels also exist between pericytes and endothelial cells at peg-socket structures providing quick communication between these cells. Specialized tight junctions between endothelial cells prevent paracellular leakage into the brain parenchyma. (**B**) At the level of penetrating arteries, upstream capillaries, endothelial cells are surrounded by vascular smooth muscle cells, and at this level of the cerebral vessels are still surrounded by the pia. The Virchow-Robin space is located between the pia and the glial limitans formed by the astrocytic endfeet. This perivascular space plays an important role in waste removal and in regulation of the interstitial fluid of the brain. *Figure reprinted with permission from (Freitas-Andrade, et al., 2020).*

1.2 Ischemic Stroke

In Canada, stroke is the third leading cause of death (Statistics Canada, 2017) and hundreds of thousands more are left with debilitating conditions after surviving a stroke (Krueger, et al., 2015). The two major classifications of stroke are ischemic and hemorrhagic (**Fig. 2**), of which ischemic stroke accounts for approximately 85% of all events, making it the most common form (Heart & Stroke Foundation of Canada, 2019). Ischemic stroke results from the narrowing or occlusion of a cerebral blood vessel caused by thrombosis or embolism of an atherosclerotic plaque, resulting in immediate local blood flow restriction to the brain (**Fig. 2B**). This is extremely detrimental for brain functionality because, unlike other organs, the brain has a limited capacity to store energy and relies on a continuous supply of substrates from blood flow (Willie, et al., 2014).

Reduced blood flow impairs the delivery of critical nutrients, particularly oxygen and glucose, subsequently restricting available energy that is required to maintain neuronal ionic gradients, resulting in failure of energy-dependent processes required for cell survival (Deb, et al., 2010). This initiates the ischemic cascade, ultimately resulting in substantial cell death in the core of the injury, an area that cannot be salvaged. Surrounding the infarct core is the peri-infarct: an area of brain tissue that is subjected to reduced blood flow that can recover if blood flow is returned within a few hours. However, if blood flow is not restored, the injured brain cells die within hours to days following the stroke, ultimately resulting in a larger and more debilitating injury that has evolved into infarction and can no longer be salvaged (Heiss, 2012; Hossmann, 2012).

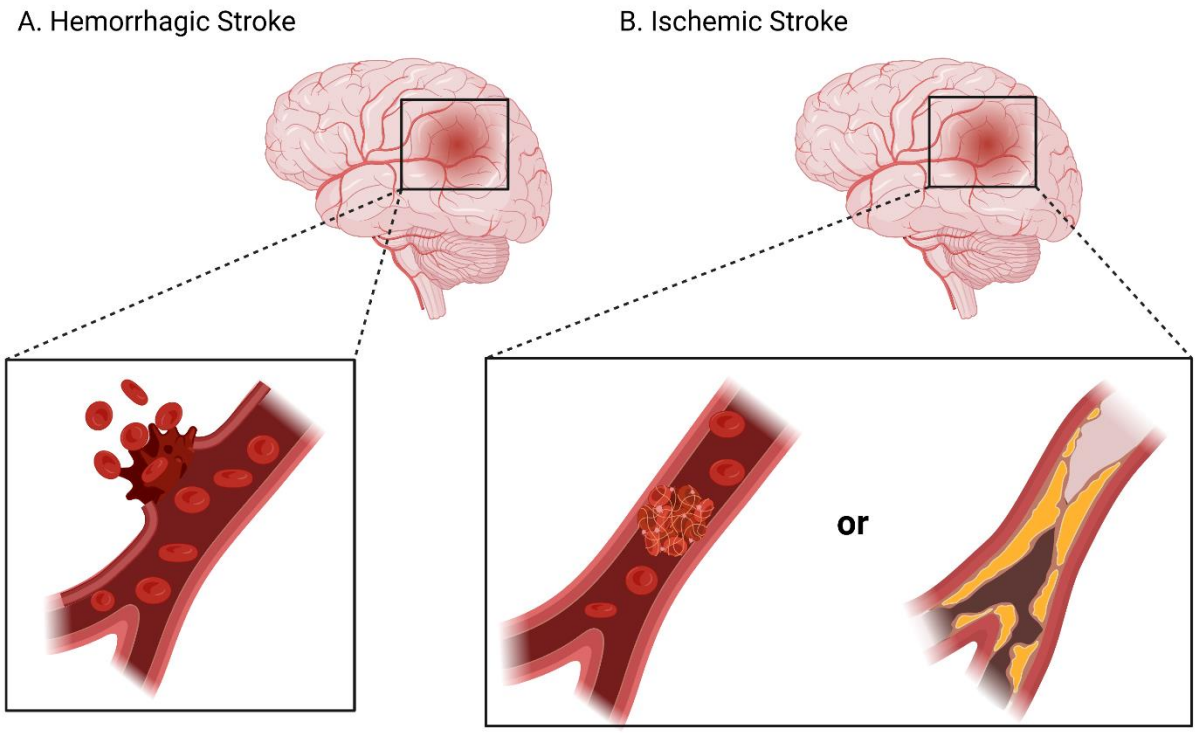

Figure 2. Major stroke classification types.

(**A**) Hemorrhagic stroke results from the rupture of a cerebral blood vessel. (**B**) Ischemic stroke results from the occlusion of a cerebral blood vessel due to a blood clot or atherosclerotic plaque. Both stroke types disrupt cerebral blood flow, thus limiting the delivery of critical nutrients to the brain to maintain proper function. *Figure created with BioRender*.

Until recently, the only effective and approved treatment for acute ischemic stroke was intravenous administration of recombinant tissue plasminogen activator (rtPA) to dissolve the obstructive clot (Hacke, et al., 2008; Hebert, et al., 2016). Acute endovascular treatment is another option to mechanically remove the clot in eligible patients, with limitations (Goyal, et al., 2015). Both therapies aim to restore perfusion to the ischemic brain as quickly as possible to maximize clinical recovery, reiterating the importance of blood flow for cerebral health (Lin & Sanossian, 2015; Prabhakaran, et al., 2015). Unfortunately, rtPA remains inaccessible to many patients because it must be administered within a narrow therapeutic window due to risk of

hemorrhagic complications, limiting its use to 10-15% of stroke victims (Iadecola & Anrather, 2011; Jauch, et al., 2013; Gurewich, 2016). Additionally, women that arrive at the hospital within the necessary time window receive rtPA treatment less when compared to men, despite evidence that women respond better to rtPA treatment (Bushnell, et al., 2018). Evidently, there is an urgent need to explore therapies that target improving perfusion with minimal associated risks to reduce disease burden and improve stroke outcomes.

1.3 Blood Flow Regulation Following Stroke

By limiting tissue perfusion, stroke affects brain homeostasis, vascular function, and compromises neuronal health (Moskowitz, et al., 2010; Tymianski, 2011; Iadecola & Anrather, 2011). There is evidence of disruption to both cerebral autoregulation and NVC during ischemic conditions (Maggio, et al., 2013; Salinet, et al., 2013; He, et al., 2020). Blood flow to the brain flows across a pressure gradient known as cerebral perfusion pressure. During ischemia, as cerebral perfusion pressure drops, cerebral autoregulation mechanisms initiate vasodilation to reduce vascular resistance in cerebral vessels and also increases peripheral blood pressure in an attempt to preserve CBF (Brouns & De Deyn, 2009; Moshayedi & Liebeskind, 2021). As cerebral perfusion pressure continues to drop, compensatory mechanisms fail, however, cells are able to maintain normal function as the average time blood stays within capillary circulation increases, therefore increasing the proportion of oxygen extracted. Eventually, cerebral metabolism reaches a plateau due to hypoxia and the onset of ischemia is established (Moshayedi & Liebeskind, 2021).

The ischemic cascade is a complex, heterogenous process resulting from bioenergetic failure due to hypoxia that involves, but is not limited to: failure of energy-dependent ion pumps,

membrane depolarization, excitotoxicity, inflammation, oxidative stress, cellular acidosis, BBB disruption, cytotoxic and vasogenic edema, and ultimately cell death (Brouns & De Deyn, 2009; Moskowitz, et al., 2010; Heiss, 2012). This disruption on the cellular and molecular level compromises the structural integrity of the cerebrovasculature. Brain ECs are distinct from those in the periphery because they express specialized tight junction proteins to regulate the passage of substances into the brain, thereby forming the BBB. Ischemia leads to a biphasic breakdown of the BBB starting with upregulation of caveolae-mediated endothelial transcytosis in the early phase, followed by tight junction protein degradation and vessel wall breakdown (Knowland, et al., 2014; Nahirney, et al., 2016; Haley & Lawrence, 2017). BBB breakdown increases vascular permeability and results in non-selective vesicular transport of blood-borne molecules across ECs, contributing to vasogenic edema.

Activation of the transcription factor hypoxia-inducible factor 1α (HIF-1α) under hypoxic conditions leads to upregulation of key angiogenic genes, including vascular endothelial growth factor (VEGF). VEGF is a potent inducer of microvascular permeability (Zhang, et al., 2002) via rapid stimulation of caveolae-mediated transcytosis (Feng, et al., 1999; Chen, et al., 2002), which is normally suppressed in the healthy brain (Tuma & Hubbard, 2003; Ben-Zvi, et al., 2014). Moreover, oxidative stress is promptly elevated in the peri-infarct region (Shi & Liu, 2007; Pradeep, et al., 2012; Rodrigo, et al., 2013) and represents a major cause of vascular dysfunction through neutralization of NO by reactive oxygen species (ROS). This decreases NO bioavailability and inhibits its modulatory role in angiogenesis and vascular reactivity (Park, et al., 2005; Fisher, 2008; Xu, et al., 2016). Interestingly, in patients with acute stroke, low NO levels following stroke correlate with outcome severity (Rashid, et al., 2003). Oxidative stress also induces vascular hyperpermeability through oxidant-induced phosphorylation of caveolin-1

and increased caveolae-mediated transcytosis in ECs in culture (Takeuchi, et al., 2013). Levels of the vasoconstrictor peptide ET-1 are also increased following stroke (Yu, et al., 2015), further exacerbating ischemia and contributing to inflammation and production of ROS, mainly superoxide O_2^- which further inhibits NO (Kowalczyk, et al., 2015). Overall, ischemia compromises both functional and structural aspects of the cerebrovasculature, contributing to the pathophysiology of neuronal death.

1.4 Hormonal Regulation of CBF

Estrogens, androgens, and their precursor dehydroepiandrosterone (DHEA) are modulators of brain perfusion (Ghisleni, et al., 2015; Boese, et al., 2017). Women have increased basal CBF values compared to men, which is mediated by 17β-estradiol (E2), the most abundant and potent estrogen in mammals (Krause, et al., 2006). E2 is the main steroid sex hormone produced by the ovaries in females, however it is also present at very low concentrations in males. When E2 binds to estrogen receptors (ERs), the production and bioavailability of nitric oxide (NO) is increased through the upregulation and activation of endothelial nitric oxide synthase (eNOS) (Miyazaki-Akita, et al., 2007), as well as decreasing the concentration of the NO-deactivating superoxide anion O^{2-} (Novella, et al., 2012). eNOS is upregulated by estrogen signalling through two pathways: (1) through classical nuclear signalling characterized by the translocation of intracellular receptors to the nucleus upon activation, followed by the binding of estrogen receptor-α (ERα) to estrogen response elements (ERE) on DNA, thereby increasing transcription of eNOS, or (2) through the activation of ERα or G-protein coupled ERs located on the cellular membrane, leading to activation of the phosphatidylinositol-3-kinase (PI3K) pathway, resulting in direct phosphorylation and activation of eNOS (Novella, et al., 2012;

Boese, et al., 2017; Simoncini, et al., 2000). Signalling through both pathways ultimately results in increased production of NO, which is a potent vasodilator of VSMCs and therefore modulates vascular tone (Chen, et al., 2008). For this reason, estrogen is said to reduce systemic blood pressure, protect against vascular disease, and increase CBF to the brain.

Testosterone is the primary sex hormone produced by the testes in males, however it is also produced by ovaries in females, albeit to a much lesser extent. Testosterone can be converted to the more potent form, dihydrotestosterone (DHT), both of which bind to androgen receptors where they act as transcription factors in most tissues, including VSMCs and ECs (Liu, et al., 2003), especially in capillary ECs in the brain (Ohtsuki, et al., 2005). Testosterone, but not DHT, can also be irreversibly converted to E2 via the enzyme aromatase (Blakemore & Naftolin, 2016). Hypertension is a vascular disease risk factor continually seen at higher rates in men compared to women (Sandberg & Ji, 2012) in which both androgen and estrogen signaling has been implicated. Hypertension pathophysiology is mediated by the renin-angiotensin system, in which estrogen supplementation has been shown to reduce signaling through this pathway, resulting in decreased levels of the potent vasoconstrictor angiotensin II and reducing peripheral blood pressure in both male and female rodents (Xue, et al., 2009; Xue, et al., 2014). The role of androgens in vascular function is far less understood, as clinical studies show protective effects of physiological androgen levels in males against hypertension, but rodent studies demonstrate vasoconstrictive properties of testosterone and upregulation of the renin-angiotensin system (Boese, et al., 2017). In terms of CBF regulation, testosterone replacement increases CBF in men with low circulating testosterone (Azad, et al., 2003), reiterating the importance of physiological androgen levels for maintaining vascular health. In women, elevated testosterone levels are associated with increased rates of hypertension (Reckelhoff, 2007), and testosterone

supplementation in post-menopausal women decreases CBF (Penotti, et al., 2001). Despite the conflicting evidence of the role of testosterone in vascular function, the consensus is that decreasing androgen levels in men associated with aging contributes to increased vascular dysfunction and disease (Boese, et al., 2017).

1.5 Hormonal Contributions to Sex Differences in Stroke

Biological sex markedly influences CBF as well as the prevalence and progression of cardiovascular diseases, including stroke (Orshal & Khalil, 2004; Krause, et al., 2006; Cosgrove, et al., 2007; Cowan, et al., 2017). It is well recognized that stroke differentially affects women and men. Although men have a higher incidence of stroke compared to age-matched pre-menopausal women, epidemiological studies show that stroke incidence dramatically increases in women following menopause (Appelros, et al., 2009; Barker-Collo, et al., 2015; Wang, et al., 2019; Bonkhoff, et al., 2021). Because women live longer than men on average, post-menopausal women have higher rates of stroke compared to age-matched men, resulting in increased mortality, worse psychological outcomes, and higher rates of disability (Turtzo & McCullough, 2010; Persky, et al., 2010; Ahnstedt, et al., 2016; Madsen, et al., 2019; Heart & Stroke Foundation of Canada, 2019). Following menopause, estrogen production by the ovaries decreases by 60 percent, which has led to the presumption that estrogen is protective against cardiovascular disease. Lower incidence rates of stroke in pre-menopausal women have been linked to a protective effect of estrogen against hypertension (Turtzo & McCullough, 2008). This is because hypertension is an independent risk factor for ischemic stroke and is more commonly seen in men (Reckelhoff, 2001). Estrogen's modulatory action on eNOS is thought to mediate this protection through promoting vasodilation and reducing vascular tone.

A neuroprotective role for estrogens has also been reported in a variety of preclinical ischemic stroke models. Numerous studies show that estrogen treatment or activation of ERs reduces lesion size in these animal models (Yang, et al., 2000; Selvaraj, et al., 2018; Xiao, et al., 2018) while removing endogenous estrogen through ovariectomy (Ovx) of female rodents worsens their outcomes (Alkayed, et al., 1998; Fukuda, et al., 2000). Even male rats that receive intravenous estrogen immediately upon reperfusion following MCAo have reduced infarct volumes compared to control-treated males (McCullough, et al., 2001). Estrogen supplementation of Ovx rodents prior to stroke has also been found to preserve BBB integrity by reducing EC death and preventing the loss of tight junction proteins (Liu, et al., 2005; Shin, et al., 2016). *In vitro*, E2 treatment protects the endothelium and increases cell survival by reducing mitochondrial ROS production following ischemic injury (Razmara, et al., 2008; Guo, et al., 2010). These protective mechanisms may contribute to preserving not only neuronal health, but also vascular health, during and following cerebral ischemia.

There are very few mechanistic investigations on disparities between sexes in post-stroke CBF outcome. Ovx rats displayed significantly lower CBF following permanent MCAo compared to intact females. Slow-release estrogen supplementation of Ovx rats given 30 minutes following stroke improved CBF values comparable to those seen in intact females, however this protective effect was not observed until 24 hours post-stroke (Yang, et al., 2000). Long-term estrogen treatment increases eNOS expression in cerebral blood vessels from male and female rats (McNeill, et al., 1999), suggesting that NO may play a protective role through vasorelaxation which requires chronic treatment to take effect. In contrast, males treated with estrogen immediately following transient MCAo had increased CBF up to 10 min following stroke, but not past 90 min (McCullough, et al., 2001), suggesting that modulation of hormones might not

be a viable therapeutic option. Only one study has shown that CBF values of female rats are higher following transient MCAo compared to males and Ovx females (Alkayed, et al., 1998), and the mechanism behind this difference has yet to be elucidated. Additionally, following a photothrombotic model of distal MCAo, female rats showed quicker vascular remodeling of occluded and peripheral vessels compared to males (Yang, et al., 2019). Overall, specific knowledge on sex differences in cerebrovascular disease is limited, and the regulation of endothelial function by sex hormones in disease states is poorly understood. Underrepresentation of the female sex in preclinical research is partly responsible for this.

Stroke recovery rates have improved markedly for men over the past 25 years, whereas recovery outcomes for women have stagnated (Silva, et al., 2010). Despite the promising effects of estrogens in rodent stroke models, hormone therapy containing either combined estrogen and progesterone, or estrogen alone, increases the risk of ischemic stroke by 40 to 50 percent in healthy postmenopausal women (Wassertheil-Smoller, et al., 2003; Hendrix, et al., 2006; Hale & Shufelt , 2015). In this case, the stroke is most often thrombotic, which is attributed to decreased plasma levels of endogenous circulating anticoagulants in response to high estrogen levels (Mendelsohn & Karas, 1999; Ritzel, et al., 2013). There is also the timing hypothesis for hormone therapy, which suggests that treatment with exogenous estrogens causes more harm when EC viability is already compromised, as is often the case in aging women (Lisabeth & Bushnell, 2012; Ritzel, et al., 2013). Additionally, hormone replacement therapy using estrogens can increase the risk of ovarian and breast cancer (Brown, et al., 2018). For these reasons, hormone replacement therapy to reduce stroke risk in post-menopausal women is not recommended. Therefore, it is critical to better understand how sex hormones regulate vascular function in order to refine future therapies.

1.6 Rho-kinase is an Important Regulator of Vascular Tone

Rho-associated coiled-coil containing protein kinase (ROCK) belongs to the family of serine-threonine kinases and is a major regulator of endothelial function through its involvement in several integral roles, including cell contractility, migration, proliferation, and regulation of the actin cytoskeleton (Riento & Ridley, 2003; Noma, et al., 2012). ROCKs are ubiquitously expressed across tissues, and their location and cell type determine its function. There are two highly homologous isoforms of ROCK: ROCK1 and ROCK2; of which the latter is primarily expressed in the brain and vasculature (Shimizu & Liao, 2014). ROCKs are downstream effectors of the family of small GTPases, including RhoA. ROCK2 is mainly localized in the cytoplasm of ECs and upon activation by GTPase-bound RhoA, is translocated to the cellular membrane. Signaling through the RhoA/ROCK pathway regulates cell contractility through ROCK's inhibitory action on myosin light chain phosphatase (MLCP). Phosphorylation of myosin light chains (MLC) initiated by elevated intracellular Ca^{2+} enables VSMC contraction, therefore removal of a phosphate group by MLCP induces relaxation (Çiçek & Ayaz, 2015; Hartmann, et al., 2015). ROCK2, the only isoform involved in the regulatory role of MLC contraction (Wang, et al., 2009), inhibits MLCP by directly phosphorylating it, therefore inhibiting dephosphorylation of MLC resulting in sustained contraction even in the absence of Ca^{2+}. Activated RhoA is also implicated in Ca^{2+} sensitization of VSMC, meaning that a lower concentration of intracellular Ca^{2+} is required to generate a contraction of equal size (Nunes & Webb, 2021).

RhoA/ROCK signaling has been implicated in the pathogenesis of various vascular diseases. Increased ROCK activity has been found in both humans with hypertension and animal models of hypertension, attributed to elevated vascular contractility and arterial wall remodeling

(Hartmann, et al., 2015; Abd-Elrahman, et al., 2015), and polymorphisms in the ROCK2 gene are associated with a lower risk of developing hypertension (Rankinen, et al., 2008). Furthermore, ROCK2 is directly involved in increased myogenic tone that is associated with aging, which may be mediated by long-term inhibition of NO availability (Nunes & Webb, 2021). ROCK has also been shown to be inhibited by insulin receptor activation and thus involved in type 2 diabetes mellitus induced vascular dysfunction (Çiçek & Ayaz, 2015) and heterozygous deletion of ROCK2 (*ROCK2*$^{+/-}$) in mice protects against high fat diet induced insulin resistance (Soliman, et al., 2012).

ROCK also influences cellular contractility by directly inhibiting phosphorylation and activation of eNOS (Ming, et al., 2002; Sugimoto, et al., 2007), as well as inhibiting eNOS expression by decreasing the stability of eNOS mRNA (Laufs & Liao, 1998). NO, the downstream effector of eNOS, negatively regulates ROCK phosphorylation and activation in cerebral ECs under normal conditions (De Silva, et al., 2016). However, hypoxia promotes soluble GC to produce inosine cyclic 3′,5'-monophosphate (cIMP) instead of cGMP (the end product of NO signaling in VSMCs), resulting in ROCK activation and MLCP inhibition (Zhao, et al., 2015). Furthermore, RhoA/ROCK signaling has been shown to be upregulated in human ECs during hypoxia, mediating downregulation of eNOS expression and activation (Takemoto, et al., 2002; Jin, et al., 2006). Pathological RhoA/ROCK2 activation in ECs also promotes the association between eNOS and caveolin-1 and their translocation to membrane caveolae compartments (Zhu, et al., 2003) where eNOS is inhibited (Ju, et al., 1997; Ming, et al., 2002) which might in turn impair BBB permeability (Allen, et al., 2010; Siddiqui, et al., 2011). Thus, ROCK signaling during ischemia may contribute to vasoconstriction and reduced blood flow in

the hypoxic region both by increasing VSMC contractility and downregulating the eNOS/NO pathway.

1.7 The Neuroprotective Role of Rho-kinase Inhibition/Deletion is Mediated by eNOS

ROCK activity has been shown to be upregulated following ischemic stroke, contributing to increased vascular permeability and enhancing oxidative stress (Shin, et al., 2007; Allen, et al., 2010; Satoh, et al., 2010; Cui, et al., 2013). Non-selective inhibition of both ROCK isoforms with fasudil reduced lesion size in male mice subjected to transient MCAo, which correlated with increased eNOS activity (Rikitake, et al., 2005). Interestingly, the neuroprotective effect of fasudil treatment was abolished in eNOS deficient (*eNOS*$^{-/-}$) mice (Rikitake, et al., 2005). Upregulation of RhoA/ROCK signaling has also been shown to increase levels of phosphorylated MLC following ischemia-reperfusion injury *in vitro*, contributing to BBB hyperpermeability, which could be attenuated by non-selective ROCK inhibitors (Allen, et al., 2010; Gibson, et al., 2014). Non-selective inhibition of ROCK by hydroxyfasudil also attenuates early BBB disruption following intracerebral hemorrhage in rats (Fujii, et al., 2012; Fu, et al., 2014). In fact, fasudil, which is metabolized to hydroxyfasudil, is the only ROCK inhibitor approved for human use in Japan and China for treatment of cerebral vasospasm following subarachnoid hemorrhage (Hartmann, et al., 2015).

Specifically pertaining to the ROCK2 isoform, selective ROCK2 inhibition with KD025 after induction of transient MCAo dose-dependently reduced infarct volume and limited perfusion loss in male mice (Lee, et al., 2014). *ROCK2*$^{+/-}$ mice, who exhibit constitutively enhanced eNOS expression and activity in brain ECs, also have reduced infarct volumes following transient MCAo compared to *ROCK1*$^{+/-}$ and wildtype mice (Hiroi, et al., 2018). These

neuroprotective effects correlated with higher levels of NO detected in the peri-infarct of *ROCK2*$^{+/-}$ mice 24 hours following transient MCAo, and neuroprotection was abolished in eNOS deficient (*eNOS*$^{-/-}$) mice (Hiroi, et al., 2018). Furthermore, the Statin class of drugs, which upregulate eNOS, have neuroprotective properties in experimental animal models of stroke (Vaughan & Delanty, 1999; Sawada & Liao, 2009). The upregulation of eNOS by Statins is mediated by inhibition of RhoA (Amin-Hanjani, et al., 2001; Tang, et al., 2017), reducing activation of RhoA's downstream effector ROCK2 (Hao, et al., 2016; Tang, et al., 2017). Altogether, these findings suggest that eNOS regulation by ROCK2 may be involved in the neuroprotective effects of ROCK2 inhibition and deletion.

1.8 Sex Differences in Rho-kinase

Agonist-mediated vasoconstriction is reduced in female rodents in response to several agonists, including serotonin (Lamping & Faraci, 2001; Nuno, et al., 2007), ET-1 (Ahnstedt, et al., 2013) and angiotensin II (Faraci, et al., 2006; Ahnstedt, et al., 2013). These sex differences in vascular reactivity have been shown to be dependent on ROCK function, both in health and disease. In aorta from male mice, contractions in response to serotonin were greater than those seen in female mice, which correlated with increased ROCK activity and could be abolished by the non-selective ROCK inhibitor Y-27632 (Nuno, et al., 2007). Furthermore, impairment of relaxation to acetylcholine in aorta from diabetic mice could be accounted for by increased RhoA/ROCK signaling in male, but not female mice (Nuno, et al., 2009). Non-selective inhibition of ROCK with H-1152 improved relaxation impairment in diabetic male mice, but had no effect on females (Nuno, et al., 2009). These results suggest that ROCK's role in Ca^{2+} sensitization may mediate sex differences in VSMC contraction.

ROCK has also been shown to contribute to sex differences specifically in cerebrovascular reactivity. In cerebral basilar arteries, the magnitude of relaxation in response to the ROCK inhibitor Y-27632 was far greater in female rats when compared to males and Ovx females (Chrissobolis, et al., 2004). Supplementing Ovx rats with 17β-estradiol treatment restored vasodilator effects of Y-27632 to those seen in intact females. Additionally, constriction in response to the eNOS inhibitor L-NAME produced significantly greater vasoconstriction in female basilar arteries compared to males, however, removal of endogenous sex hormones by Ovx did not alter this response (Chrissobolis, et al., 2004). Another study showed that constriction of basilar arteries in response to angiotensin II was greater in male mice compared to females (Faraci, et al., 2006). Angiotensin II-induced vasoconstriction could also be selectively abolished by Y-27632, suggesting that ROCK mediates this response. Together, these findings show that both peripheral and cerebral vasoreactivity is mediated by ROCK in a sex-dependent manner.

Interestingly, there is some evidence that estrogen may increase ROCK activity in females. Superior mesenteric arteries isolated from rats showed greater constriction in response to norepinephrine in young adult female rats aged 8-24 weeks, but not in adolescent (4 week) or aged (1 and 1.5 years) female rats. This increased vascular reactivity correlated with increased estrogen levels in young adult females (Li, et al., 2014). Furthermore, protein levels of ROCK were significantly greater in mesenteric arteries from both young adult and aged female rats compared to age-matched males. Short-term incubation with estrogen increased ROCK activity in mesenteric arteries, and long-term incubation increased protein levels of ROCK, suggesting both genomic and non-genomic regulation of ROCK by estrogen (Li, et al., 2014). Another study found increased levels of activated RhoA and phosphorylated MLC in human platelets from

women, suggesting that increased ROCK activity in females may account for the reported platelet hyperreactivity (Schubert, et al., 2016). Low testosterone observed with aging and vascular disease in males is also associated with the upregulation of ROCK (Sopko, et al., 2014), however further studies are warranted to decipher the precise mechanisms involved.

1.9 Rationale and Hypothesis

The neuroprotective role of ROCK inhibition and deletion following stroke has been well characterized, presumably by indirectly increasing NO bioavailability. Despite NO being a potent vasodilator and regulator of CBF, the role of ROCK in CBF outcomes following stroke has yet to be fully characterized. It is now well recognized that stroke differentially affects women and men, however, overrepresentation of male subjects in preclinical research has left many questions unanswered. The mechanisms underlying cerebrovascular stroke outcomes are poorly understood, and the effects of sex hormones on cerebrovascular regulation in the ischemic brain have yet to be fully comprehended. Considering the overlapping roles of hormonal and rho-kinase regulation of vascular function (**Fig. 3**), this research project aims to address the overarching hypothesis that ROCK2 is involved in CBF outcomes following a focal ischemic stroke in a sex-specific manner. Elucidating the cellular and molecular bases of sex differences in cerebrovascular pathophysiology is vital for understanding the nature and origins of stroke outcomes, and for designing novel therapeutic strategies to promote functional recovery in both women and men.

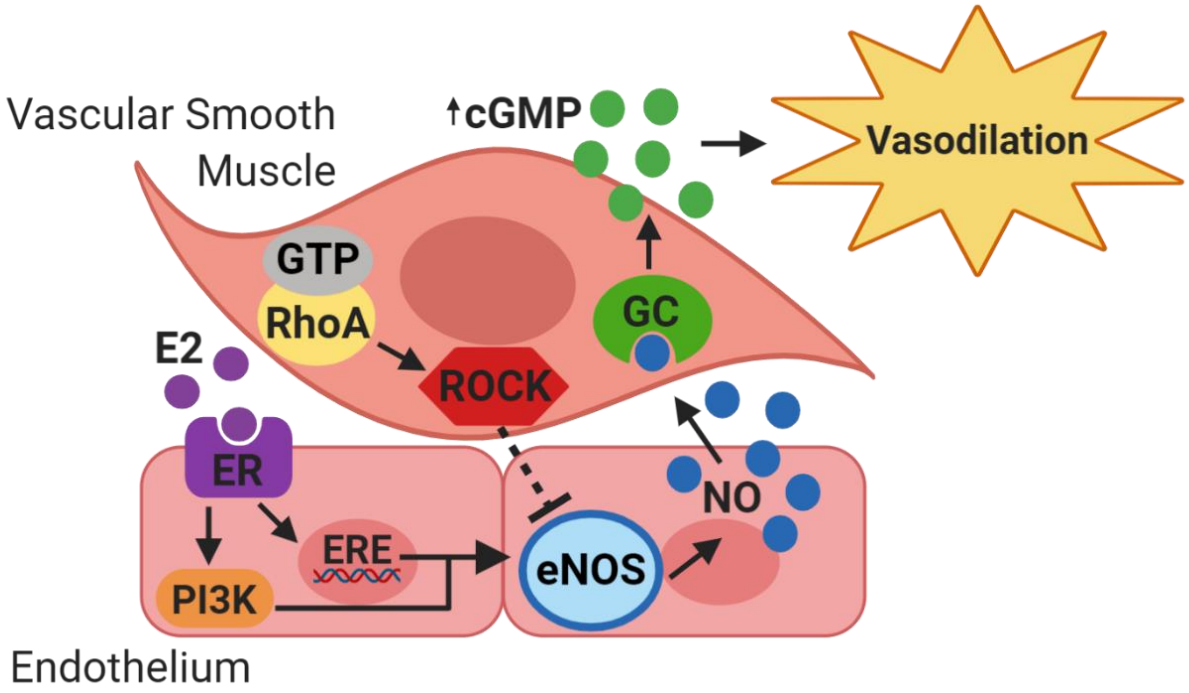

Figure 3. Converging roles of estrogen and rho-kinase signalling on endothelial nitric oxide synthase (eNOS) regulation.

When 17β-estradiol (E2) binds to estrogen receptors (ER), signaling through several receptor-specific pathways leads to upregulation of endothelial nitric oxide synthase (eNOS). E2 binding to ERα leads to classical nuclear signaling involving translocation of ERα to the nucleus where it binds to estrogen response elements (ERE) and acts as a transcription factor, inducing transcription of eNOS mRNA. Intracellular signaling of E2 when bound to ERα or G-protein coupled ER leads to signaling through the phosphatidylinositol-3-kinase (PI3K) pathway, resulting in phosphorylation and activation of eNOS. Activation of eNOS results in nitric oxide (NO) production, which stimulates soluble guanylyl cyclase (GC) in nearby vascular smooth muscle cells to produce cyclic guanosine monophosphate (cGMP), resulting in vasodilation via activation of protein kinase G. Rho-kinase (ROCK), induced to its active conformation by binding of GTP-bound active RhoA, inhibits expression of eNOS by decreasing the stability of eNOS mRNA. ROCK also decreases eNOS activation by directly preventing eNOS phosphorylation. Overall, signaling through ERs results in increased bioavailability of NO, a potent vasodilator, while signalling through the RhoA/ROCK pathway decreases NO bioavailability. *Figure created with BioRender.*

2. Methods

2.1 Subjects

Male and female *ROCK2*$^{+/-}$ mice and wild-type (WT) littermates were bred in house and housed a maximum of five per cage with free access to food and water. Animals were maintained on Teklad Global 18% Protein Rodent Diet (Harlan Laboratories, Teklad Diets, Madison WI) composed of 18.6% protein, 6.2% fat, 3.5% fiber and 44.2% carbohydrates. Mice were aged 8-10 weeks when experimental procedures were initiated. All methods and procedures were approved by the University of Ottawa's Animal Care Committee and are in accordance with the Canadian Council on Animal Care guidelines.

2.2 Female Gonadectomy

All female mice received either a sham surgery (referred to herein as "intact females") or a bilateral ovariectomy (Ovx). Mice were initially anesthetized with 4% isoflurane and then maintained at 2.5% isoflurane for the duration of the surgery. The back of the mouse was shaved, skin disinfected, and slow-release buprenorphine (1.2mg/kg, Chiron Compounding Pharmacy Inc., Guelph, ON, Canada) and 1mL of saline (0.9%) were both administered subcutaneously (SC) prior to performing the surgery. The mouse was then placed on a pad heated to 37°C and positioned in sternal recumbency. Using a sterile scalpel, a 1-cm incision was made down the midline of the lower back. The skin was then gently separated using a blunt probe and the ovary was visualized near the flanks, where it is attached to adipose tissue. A small incision was made in the abdominal wall, and the adipose tissue was gently pulled out of the intraperitoneal cavity along with the ovary attached. A clamp was placed just below the ovary at the uterine horn and held in place for 5-10 seconds, followed by excision of the ovary. The clamp remained in place

for an additional 5-10 seconds after excision to reduce bleeding. Once the clamp was released, the adipose tissue was returned to the peritoneal cavity and the abdominal incision was sutured closed. This exact procedure was performed again on the opposite side to remove both ovaries. Finally, the midline incision in the back was closed with autoclips and topical bupivacaine (bupivacaine hydrochloride as monohydrate, 2%, Chiron Compounding Pharmacy Inc., Guelph, ON, Canada) was applied to the incision site for analgesia. Mice were placed in a 37°C chamber until they woke up and were then returned to a clean home cage. Mice were monitored 4 hours following the procedure and for the following 3 days in the morning to ensure proper recovery. Sham Ovx surgery was performed exactly as above, without clamping or excision of the ovaries. Mice were allowed to recover for 10-14 days before any further experimental procedures were performed.

2.3 Male Gonadectomy

All male mice received either a sham surgery (referred to herein as "intact males") or gonadectomy (Gdx) to remove both testicles. Mice were initially anesthetized with 4% isoflurane and then maintained at 2.5% isoflurane for the duration of the surgery. The scrotum of the mouse was shaved, skin disinfected, and carprofen (20mg/kg, Rimadyl®, Zoetis Canada Inc., Kirkland, QC, Canada) and 1mL of saline (0.9%) were both administered SC prior to performing the surgery. The mouse was then placed on a pad heated to 37°C and positioned in dorsal recumbency. A 1-cm incision was made down the midline of the scrotum and the tunica was gently separated from the skin using a blunt probe. Gentle pressure was applied to the lower abdomen of the mouse to push out both testes. A clamp was then placed on the adipose tissue visible just above the testes to restrict blood flow. After approximately 10 seconds, a size 4-0

suture was tied loosely around the tissue behind the clamp. The clamp was then released, the knot was checked to ensure no skin was caught, and then the knot was tied tightly around the tissue. The testes were clamped one more time in front of the knotted suture and then both testicles were excised. The clamp remained in place for another 5-10 seconds. After removing the clamp, the excision site was monitored for any bleeding and then the incision site was closed with size 6-0 sutures. Topical bupivacaine (2%) was applied to the incision site for analgesia and mice were placed in a 37°C chamber until they woke up and were then returned to the home cage. Mice were monitored for 4 hours following the procedure and for the following 2 days in the morning to ensure proper recovery. Mice also received a second SC dose of carprofen (20mg/kg) the morning following the procedure for analgesia. Sham Gdx surgery was performed exactly as above, without clamping, tying off, or excision of the testes. Mice were allowed to recover for 10-14 days before any further experimental procedures were performed.

2.4 Laser Doppler Flowmetry and Photothrombotic Stroke

Cerebral blood flow was measured using laser doppler flowmetry (LDF, transonic® tissue perfusion monitor) in the somatosensory cortex under ketamine (100mg/kg, Vétoquinol N.-A. Inc., Lavaltrie, QC, Canada) and xylazine (10mg/kg, Nerfasin 20™, Dechra Regulatory B. V., Bladel, The Netherlands) anesthesia (K/X) administered SC as a bolus dose. A top up dose of ketamine (25mg/kg) and xylazine (2.5mg/kg) was administered SC as a maintenance dose approximately 30 minutes following the initial dose. Animal temperature was maintained with a feedback-controlled rectal thermometer and heating pad system (Harvard Apparatus Homeothermic Monitoring System, Holliston, MA, USA) at 37°C ± 1°C. After a sufficient anesthetic plane was reached, the mouse was placed in a stereotaxic frame and an incision was

made down the midline of the skull. A high-speed microdrill was then used to thin the skull to translucency at the following coordinates relative to bregma: -2.7 anterior-posterior, +4 medial-lateral. At these coordinates, an LDF probe was placed just above the skull at a 25° angle to measure blood flow. The LDF technique uses a probe comprised of a laser of a specific monochromatic wavelength and a detector. The laser is reflected off red blood cells and the backscattered light creates an interference pattern on the detector surface, which measures the doppler shift of red blood cells as they pass and provides a relative measure of perfusion (Fredriksson, et al., 2007). While LDF does not give an absolute measurement of perfusion, it has high temporal resolution to measure rapid relative changes in perfusion, which can be measured reliably over time (Tajima, et al., 2014). To induce photothrombotic (PT) stroke, mice received an intraperitoneal injection of the photosensitive dye rose bengal (RB, 100mg/kg, MilliporeSigma: Cat. No. R3877) dissolved in phosphate buffered saline (PBS). RB was allowed to circulate for 5 minutes, during which baseline LDF measurements were taken. At the end of the 5-minute period, a 532nm laser was turned on for 10 minutes at a distance of 3-cm from the skull at the same coordinates used for LDF measurements. Photoactivation of the light-sensitive RB results in production of singlet oxygen leading to endothelium damage and platelet aggregation forming a thrombus (Lee et al., 2007). Post-stroke LDF measurements were then taken at the same coordinates for 30 minutes. Post-stroke blood flow measurements were normalized to baseline for each individual mouse for statistical analysis. At the end of the procedure, mice received a dose of buprenorphine (0.1mg/kg, Vetergesic® buprenorphine hydrochloride, Ceva Animal Health Inc., Cambridge, ON, Canada) administered SC for analgesia and 1.5mL of SC saline (0.9%) to rehydrate the animal. Finally, topical bupivacaine

(2%) was applied to the incision site for analgesia and mice were left in a 30°C incubator for approximately 4 hours until the anesthesia had worn off and normal activity resumed.

2.5 Follow up Laser Doppler Flowmetry

Additional 30-minute LDF measurements were taken at 48-hours and 1-week post-stroke. Mice were anesthetized with ketamine (100mg/kg) and xylazine (10mg/kg) anesthesia, with no maintenance dose being required. Mice were again placed in a stereotaxic frame and an LDF probe was placed at a 25° angle at the same coordinates used for all previous LDF measurements and PT stroke induction: -2.7 anterior-posterior, +4 medial-lateral. No additional thinning of the skull was performed. Animal temperature was maintained with a rectal thermometer and heating pad at 37°C ± 1°C. At the end of the procedure, mice received 1.5mL of SC saline (0.9%), topical bupivacaine (2%) was applied to the incision site, and mice were left in a 30°C incubator to recover for 4 hours.

2.6 Infarct Volumes

For quantification of infarct volumes, in-vivo magnetic resonance imaging (MRI) was performed 48 hours after PT stroke induction using a 7 Tesla GE/Agilent MR (University of Ottawa pre-clinical imaging core facility). Mice were anesthetized for the MRI procedure using 2% isoflurane. A 2D fast spin echo sequence (FSE) pulse sequence was used for the imaging, with the following parameters: slice thickness=0.5 mm, spacing=0 mm, field of view=2.5 cm, matrix=256x256, echo time=41 ms, repetition time=7000 ms, echo train length=8, bandwidth=16 kHz, fat saturation. Stroke lesions demonstrated hyperintensity. MRI images were loaded in the

Fiji software (https://imagej.net/software/fiji/) and infarct volumes were quantified using a custom script for outlining the infarct perimeter. All infarct volumes were quantified twice to obtain an average of the two measures for each animal. Subsequent LDF measurements for this timepoint were taken at least 1 hour following isoflurane exposure.

2.7 Nitric Oxide Stain

PT stroke was performed as outlined in section 2.4 above. 24 hours following stroke induction, mice were sacrificed using cervical dislocation followed by decapitation and brains were extracted and placed in ice-cold 1xPBS. A brain matrix placed on ice was used to cut 2-mm sections of tissue that encompassed the infarcted tissue. Brain slices were incubated in the dark with 5µmol of DAF-FM diacetate stain (Invitrogen by ThermoFisher, cat# D23844) diluted in 1xPBS for 20 minutes followed by a 1xPBS wash with DAPI [1:20 000] for 5 minutes. A final 1xPBS wash was performed for at least 10 minutes prior to being imaged. Just before imaging, the slice was removed from solution and placed on a microscope slide for imaging using a Zeiss Axio Imager M2 microscope equipped with a digital camera (Axiocam 506 mono) at 5X objective. DAPI was excited with 461nm and DAF-FM diacetate was excited using 594nm wavelength. Using Fiji software (https://imagej.net/software/fiji/), infarcted tissue was outlined with the polygon tool on the DAPI channel only. This outline was then saved as a region of interest (ROI) and loaded directly onto the same image with only the DAF-FM stain and the mean grey value for the entire ROI was calculated by the software. The ROI was then positioned on the same brain slice on the hemisphere contralateral to the lesion and in a corresponding area of the cortex and the mean grey value for the DAF-FM stain was also taken. Mean grey value

from the ROI on the contralateral side was subtracted from the mean grey value of the infarcted tissue and this is the value that was used for analysis.

2.8 Statistical Analysis

LDF measurements provided continuous CBF measurements over the selected region. To analyze post-stroke CBF values, measurements were normalized to pre-stroke baseline values after RB was injected, but before laser illumination. To do this, the percent change in CBF was measured by taking each post-stroke data point and dividing it by the mean of the entire 4-minute baseline recording, and multiplying that value by 100%. Each baseline data point was also divided by the mean of the entire 4-minute baseline recording and multiplied by 100%. Therefore, normalized pre-stroke baseline values are always 100%, and post-stroke values measure the change in CBF from baseline values. Statistical analyses were performed using GraphPad Prism software (version 9.2.0). Hyperacute timepoints were analyzed using a repeated measures 2-way ANOVA. Due to animal loss, comparisons of 48-hour and 1 week data points were analyzed using a 2-way ANOVA.

3. Results

3.1 Sex Differences in CBF Values Following a PT Stroke in the Somatosensory Cortex

Following PT stroke in the somatosensory cortex, CBF averaged over the 30-minute period dropped to 85.13% ± 2.48 (mean ± SD) of baseline values in Intact WT males, while Intact WT females dropped to 62.78% ± 2.75. There was no significant difference between these groups in average CBF values in the first 30 minutes post stroke (**Fig. 4C**). Although there was

no significant difference in CBF values between overall CBF values post-stroke, the individual curves for each group (**Fig. 4A**) show a phenotypic difference between groups. Intact WT females show an immediate reduction in CBF and stay relatively stable throughout the 30-minute recording, whereas Intact WT males show a noticeably sloped delay in CBF drop. Because of this apparent separation between groups at the beginning of the CBF values post-stroke, we broke up the 30-minute time period into smaller sections, herein referred to as "hyperacute timepoints". The most noticeable difference between groups was during the first 0-5 minutes following stroke, where Intact WT males had mean normalized CBF values of 88.60% ± 27.73 and Intact WT females averaged 59.34% ± 19.47, however there was no statistical significance between groups (p=0.0635). There were no differences between groups at any other hyperacute timepoint (**Fig. 4B**). Interestingly, when measured at 48 hours following stroke, Intact WT males showed a significant decrease in CBF values compared to the values taken immediately post-stroke (**Fig. 4B**). A further drop in CBF values was not observed in Intact WT females, and there were no differences within or between groups at the 1-week timepoint (**Fig. 4B**).

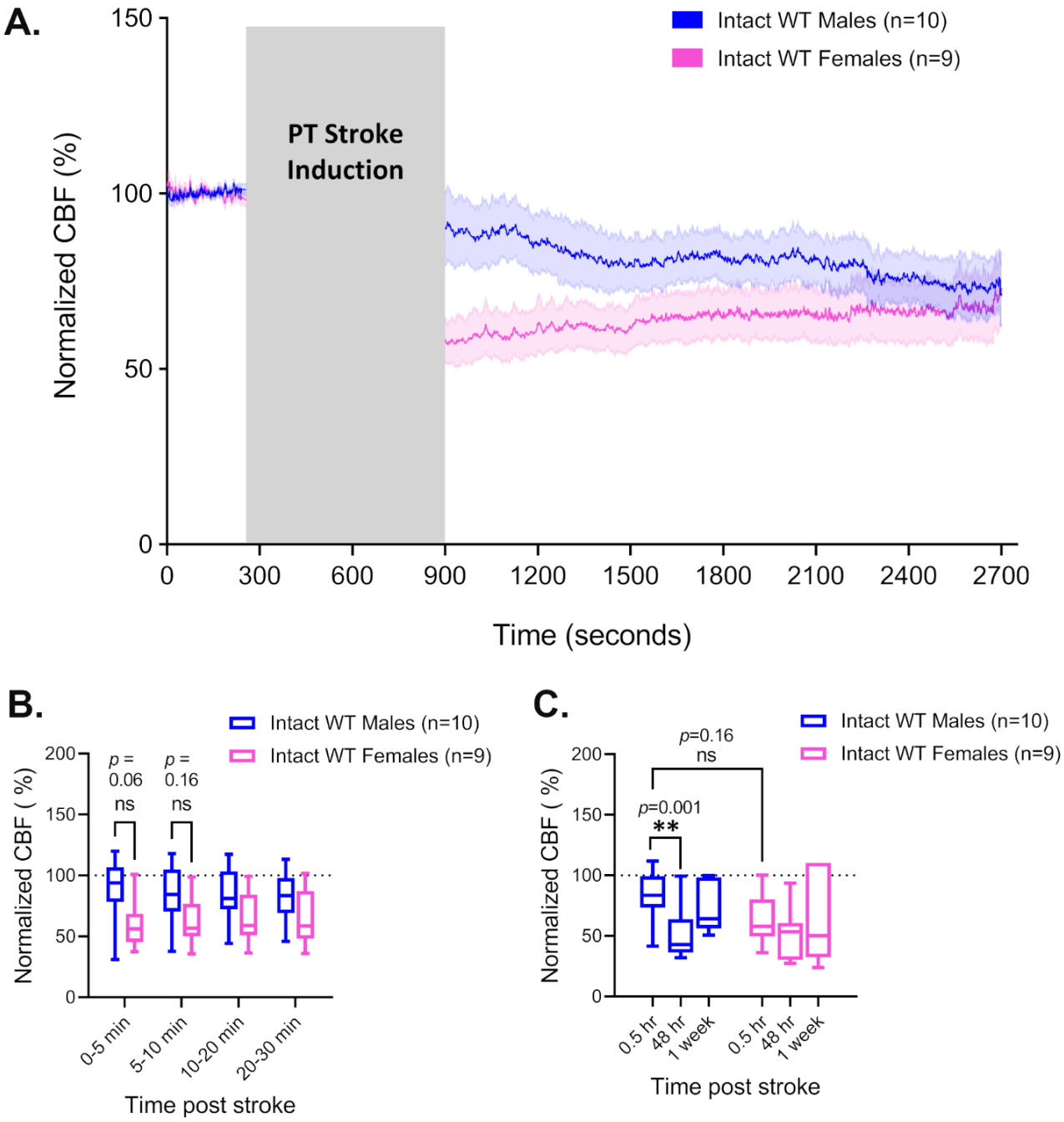

Figure 4. CBF in Intact WT males vs. females post PT stroke in the somatosensory cortex.

(**A**) CBF measured by LDF under K/X anesthesia in intact WT male and intact WT female mice before and after a PT stroke. Grey box indicates time passed during laser irradiation of the PT stroke induction. Post-PT values are normalized to pre-PT baseline values. Curved lines represent average normalized CBF of all animals in the respective group. Shaded area above and below curves represent SEM. (**B**) Averaged CBF measurements of hyperacute timepoints during the 30 minutes immediately following PT stroke induction shown in A. Bars represent min to max values with a line at the mean ± SD. (**C**) Averaged 30-minute recordings of normalized CBF measured immediately post stroke (0.5hr), 48 hours post PT, and 1 week post PT. Bars represent min to max values with a line at the mean ± SD.

3.2 The Contribution of Endogenous Sex Hormones to Observed Sex Differences in CBF Following PT Stroke

To determine the role of endogenous sex hormones on CBF outcomes following stroke, mice were gonadectomized prior to receiving a PT stroke, and CBF values were compared to intact mice that received a control sham surgery. Gdx WT male mice did not show any differences in CBF values compared to Intact WT males at any hyperacute timepoint following stroke (**Fig. 5A,B**). Furthermore, as observed in Intact WT males, Gdx WT males also showed a significant decrease in CBF values at 48 hours post-stroke when compared to immediate post-stroke values (**Fig. 5C**). There were no differences in CBF values within or between groups at the 1-week timepoint (**Fig. 5C**).

CBF values in Ovx WT females dropped to an average of 80.22% ± 20.64 compared to baseline values during the full 30-minute post-stroke period. This is higher than was observed in Intact WT females, although the difference was not statistically significant (**Fig. 6C**). Although there is separation between the CBF curves immediately post-stroke (**Fig. 6A**), there was no significant difference in CBF values between groups at any of the hyperacute timepoints (**Fig. 6B**). Interestingly, similarly to what was observed in Intact and Gdx WT males, Ovx WT females also showed a significant decrease in CBF values measured at 48 hours post-stroke compared to those measured immediately post-stroke (**Fig. 6C**). There were no differences in CBF values within or between groups at the 1-week timepoint (**Fig. 6C**).

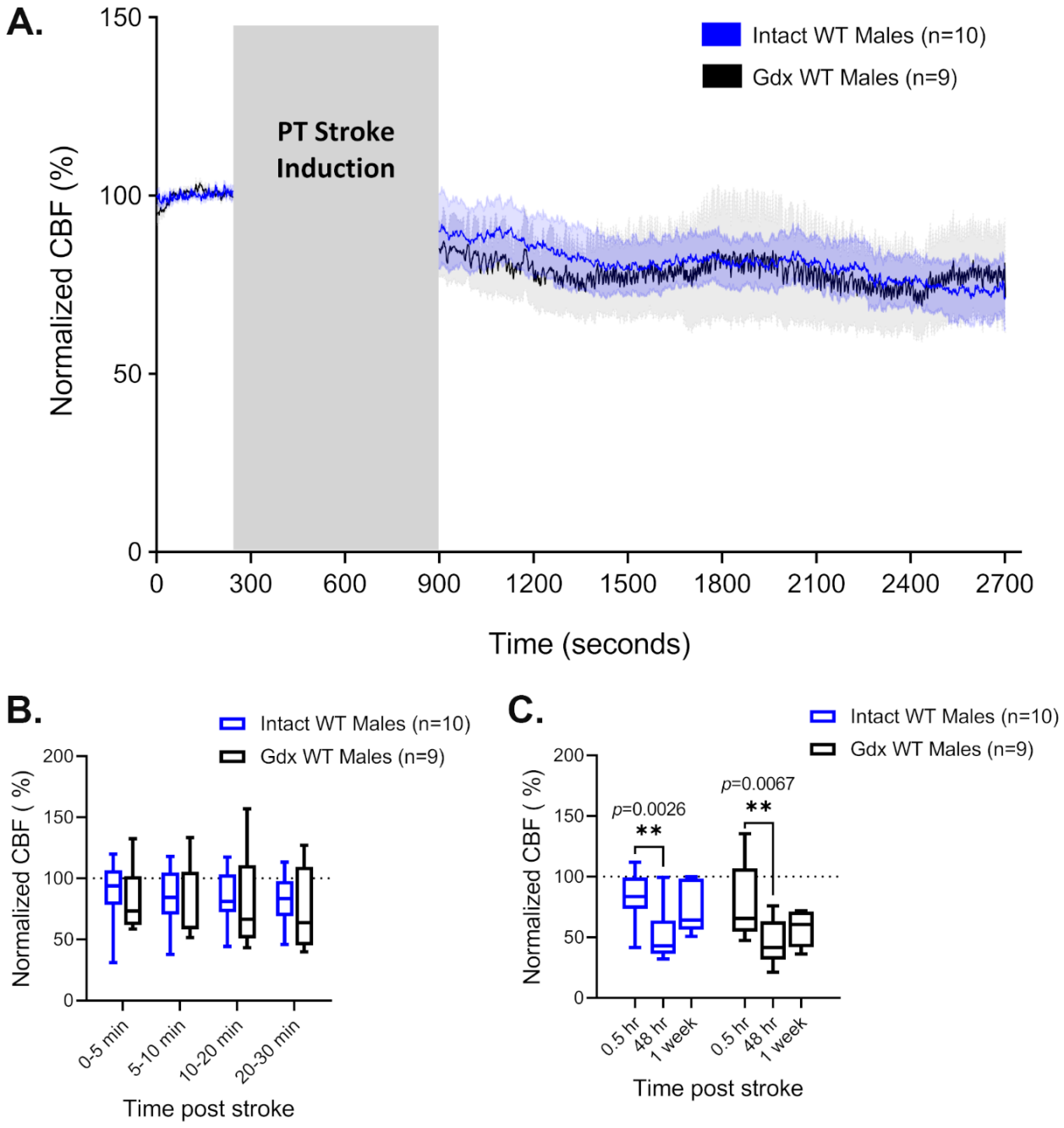

Figure 5. Removing endogenous male sex hormones does not change CBF outcomes post PT stroke.

(**A**) CBF measured by LDF under K/X anesthesia in Intact WT male and Gdx WT male mice before and after a PT stroke. Grey box indicates time passed during laser irradiation of the PT stroke induction. Post-PT values are normalized to pre-PT baseline values. Curved lines represent average normalized CBF of all animals in the respective group. Shaded area above and below curves represent SEM. (**B**) Averaged CBF measurements of hyperacute timepoints during the 30 minutes immediately following PT stroke induction shown in A. Bars represent min to max values with a line at the mean ± SD. (**C**) Averaged 30-minute recordings of normalized CBF measured immediately post stroke (0.5hr), 48 hours post PT, and 1 week post PT. Bars represent min to max values with a line at the mean ± SD.

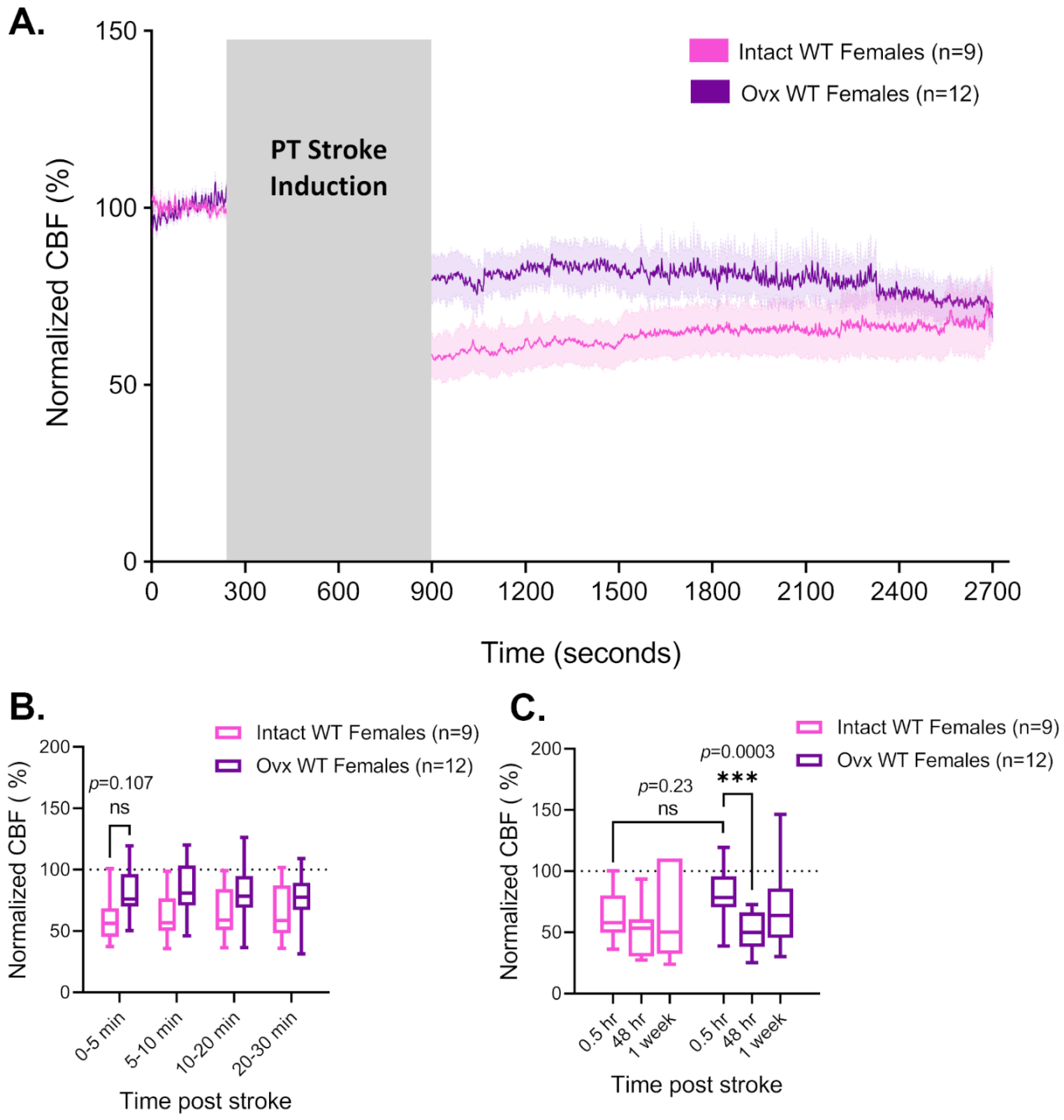

Figure 6. The effects of removing endogenous female sex hormones on CBF outcomes following stroke.

(**A**) CBF measured by LDF under K/X anesthesia in Intact WT female and Ovx WT female mice before and after a PT stroke. Grey box indicates time passed during laser irradiation of the PT stroke induction. Post-PT values are normalized to pre-PT baseline values. Curved lines represent average normalized CBF of all animals in the respective group. Shaded area above and below curves represent SEM. (**B**) Averaged CBF measurements of hyperacute timepoints during the 30 minutes immediately following PT stroke induction shown in A. Bars represent min to max values with a line at the mean ± SD. (**C**) Averaged 30-minute recordings of normalized CBF measured immediately post stroke (0.5hr), 48 hours post PT, and 1 week post PT. Bars represent min to max values with a line at the mean ± SD.

3.3 Sex-specific Outcomes of ROCK2 Haploinsufficiency on CBF Values Following PT stroke

Intact *ROCK2*$^{+/-}$ male mice did not show any differences in CBF values compared to Intact WT males at any hyperacute timepoint following stroke (**Fig. 7A,B**). Furthermore, as observed in Intact WT males, Intact *ROCK2*$^{+/-}$ males also showed a significant decrease in CBF values at 48 hours post-stroke when compared to immediate post-stroke values (**Fig. 7C**). There were no differences in CBF values within or between groups at the 1-week timepoint (**Fig. 7C**). This suggests that ROCK2 haploinsufficiency in males does not alter CBF outcomes following a PT stroke in the somatosensory cortex.

Intact *ROCK2*$^{+/-}$ females had significantly higher CBF values immediately following stroke compared to Intact WT females when averages for the entire 30-minute timepoint were compared (**Fig. 8A,C**). Surprisingly, when this timepoint was broken up into smaller hyperacute timepoints, there was no difference between groups at any of the hyperacute timepoints (**Fig. 8B**). Intact *ROCK2*$^{+/-}$ females also showed a significant decrease in CBF values at 48 hours post-stroke when compared to immediate post-stroke values (**Fig. 8C**). There were no differences in CBF values within or between groups at the 1-week timepoint (**Fig. 8C**).

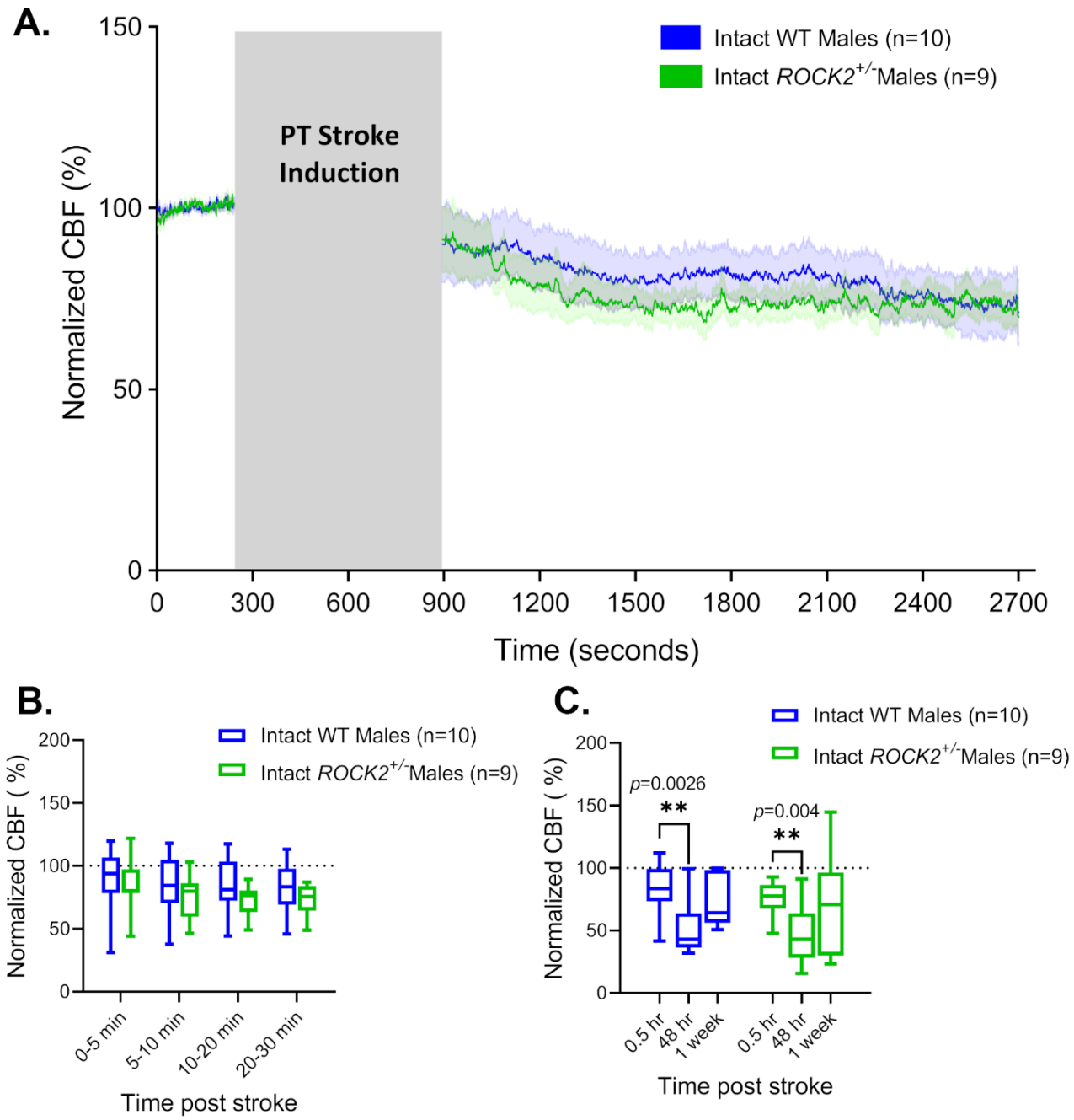

Figure 7. ROCK2 haploinsufficiency does not alter CBF outcomes in males following PT stroke in the somatosensory cortex.

(**A**) CBF measured by LDF under K/X anesthesia in Intact WT male and Intact *ROCK2*$^{+/-}$ male mice before and after a PT stroke. Grey box indicates time passed during laser irradiation of the PT stroke induction. Post-PT values are normalized to pre-PT baseline values. Curved lines represent average normalized CBF of all animals in the respective group. Shaded area above and below curves represent SEM. (**B**) Averaged CBF measurements of hyperacute timepoints during the 30 minutes immediately following PT stroke induction shown in A. Bars represent min to max values with a line at the mean ± SD. (**C**) Averaged 30-minute recordings of normalized CBF measured immediately post stroke (0.5hr), 48 hours post PT, and 1 week post PT. Bars represent min to max values with a line at the mean ± SD.

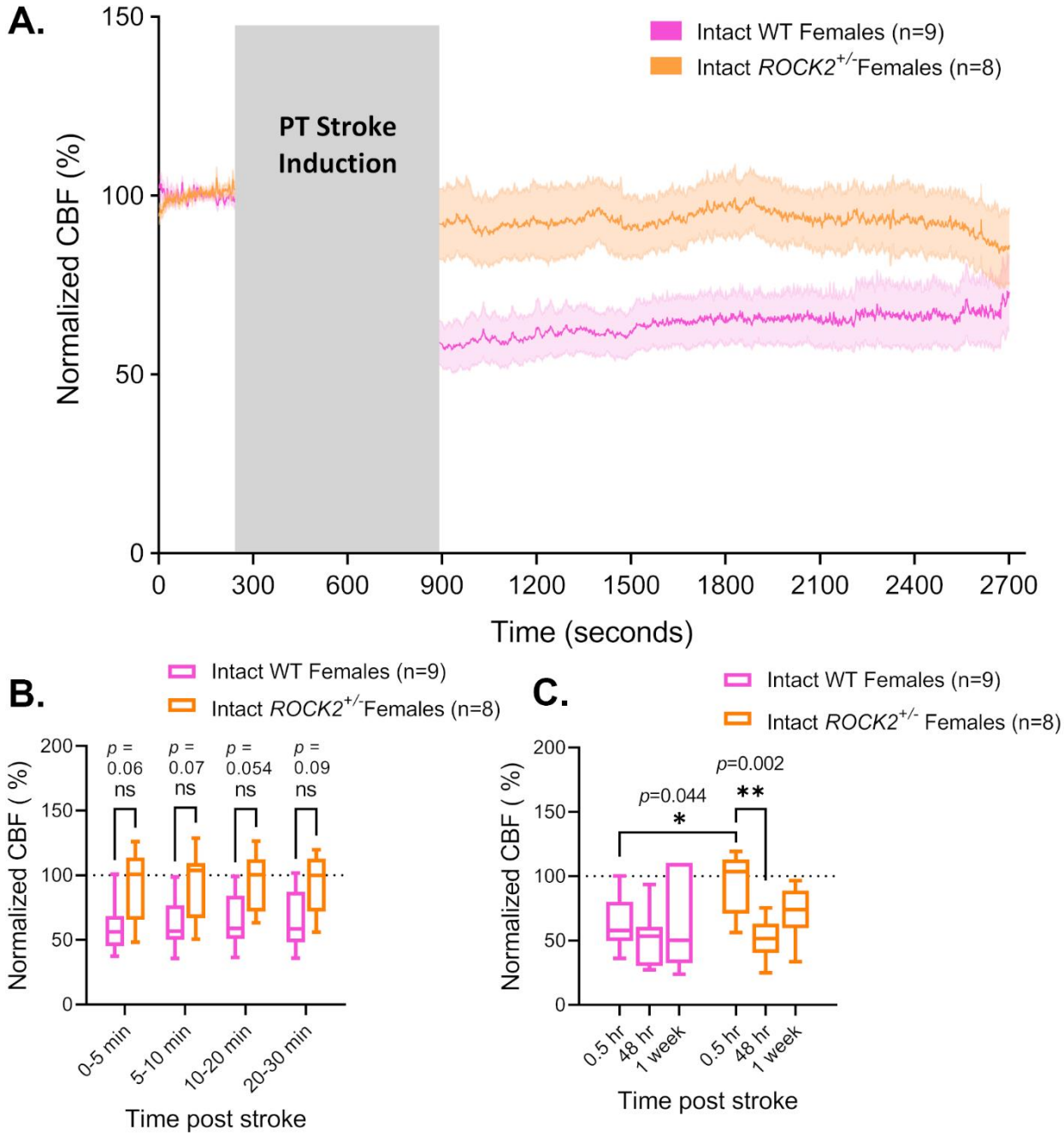

Figure 8. The effects of ROCK2 haploinsufficiency on CBF outcomes in females following PT stroke in the somatosensory cortex.

(**A**) CBF measured by LDF under K/X anesthesia in Intact WT female and Intact *ROCK2*$^{+/-}$ female mice before and after a PT stroke. Grey box indicates time passed during laser irradiation of the PT stroke induction. Post-PT values are normalized to pre-PT baseline values. Curved lines represent average normalized CBF of all animals in the respective group. Shaded area above and below curves represent SEM. (**B**) Averaged CBF measurements of hyperacute timepoints during the 30 minutes immediately following PT stroke induction shown in A. Bars represent min to max values with a line at the mean ± SD. (**C**) Averaged 30-minute recordings of normalized CBF measured immediately post stroke (0.5hr), 48 hours post PT, and 1 week post PT. Bars represent min to max values with a line at the mean ± SD.

3.4 Interactions Between Sex Hormones and ROCK2 in CBF Outcomes Following PT Stroke

There were no differences in CBF values in the total averages or in separated hyperacute timepoints between male and female Intact ROCK2$^{+/-}$ mice following PT stroke (**Fig. 9A,B**). Both Intact *ROCK2*$^{+/-}$ males and females showed a significant decrease in CBF values at 48-hours post stroke compared to immediate post-stroke values, with no other differences at any other timepoint (**Fig. 9C**). Removal of male endogenous sex hormones did not change the CBF response in the hyperacute phase following stroke in Gdx *ROCK2*$^{+/-}$ males compared to Intact *ROCK2*$^{+/-}$males (**Fig. 10A,B**). As observed in Intact *ROCK2*$^{+/-}$ males, Gdx *ROCK2*$^{+/-}$ males also showed a decrease in CBF values measured 48 hours post-stroke compared to those measured immediately post-stroke, although this was not statistically significant (p=0.139, **Fig. 10C**). There were no other differences in CBF values between or within groups at the 1-week timepoint (**Fig. 10C**). Removal of endogenous female sex hormones also did not change the CBF response following PT stroke in the hyperacute phase in Ovx *ROCK2*$^{+/-}$ females compared to Intact *ROCK2*$^{+/-}$ females (**Fig. 11A,B**). Both Intact and Ovx *ROCK2*$^{+/-}$ females showed significantly reduced CBF values at 48 hours following PT stroke compared to values measured immediately following PT stroke (**Fig. 11C**). There were no other differences in CBF values between or within groups at the 1-week timepoint (**Fig. 11C**).

Contrary to what was observed in WT mice, removal of endogenous hormones prior to stroke induction in *ROCK2*$^{+/-}$ mice did not alter CBF outcomes in either males (**Fig. 12**) or females (**Fig. 13**). Gdx *ROCK2*$^{+/-}$ males displayed the same gradual decline in the first 0-5 minutes post stroke as Intact *ROCK2*$^{+/-}$ males (**Fig. 12A**), and there were no differences between groups at any hyperacute timepoint (**Fig. 12B**). Gdx *ROCK2*$^{+/-}$ males also displayed the same delayed drop in CBF values, reaching maximum CBF deficit when measured at 48 hours

following stroke induction, although not statistically significant when compared to immediate post-stroke values (**Fig. 12C**). When compared to Intact *ROCK2*$^{+/-}$ females, there were no differences in CBF values in the hyperacute phase in Ovx *ROCK2*$^{+/-}$ females (**Fig. 13A,B**). Both groups also showed a maximum drop in CBF at 48 hours post-PT which was significantly different from immediate post-PT values (**Fig. 13C**). There were no other differences in CBF values between or within groups at the 1-week timepoint (**Fig. 13C**).

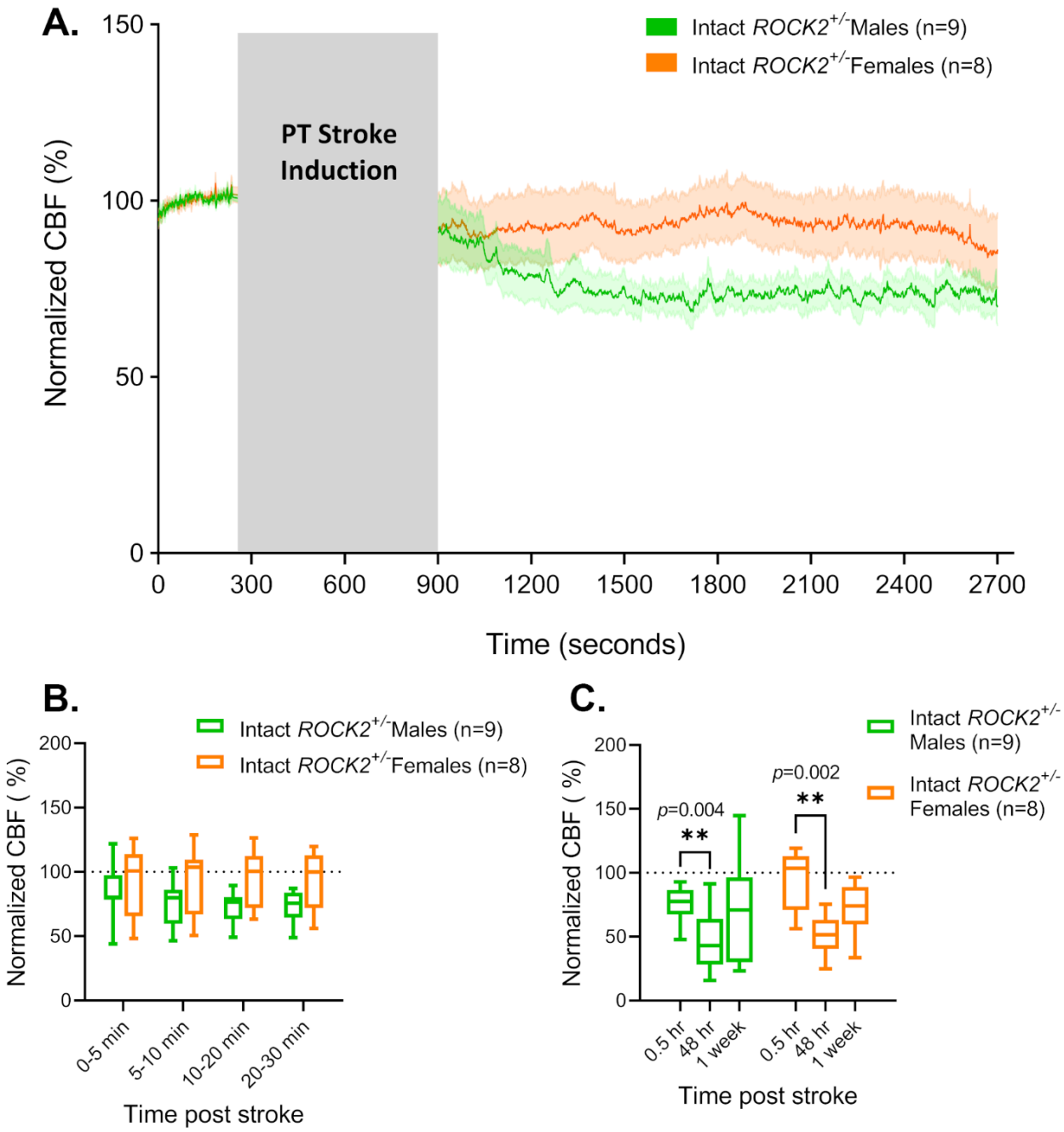

Figure 9. CBF in Intact *ROCK2*$^{+/-}$ male vs. female mice post PT stroke in the somatosensory cortex.

(**A**) CBF measured by LDF under K/X anesthesia in Intact *ROCK2*$^{+/-}$ male and Intact *ROCK2*$^{+/-}$ female mice before and after a PT stroke. Grey box indicates time passed during laser irradiation of the PT stroke induction. Post-PT values are normalized to pre-PT baseline values. Curved lines represent average normalized CBF of all animals in the respective group. Shaded area above and below curves represent SEM. (**B**) Averaged CBF measurements of hyperacute timepoints during the 30 minutes immediately following PT stroke induction shown in A. Bars represent min to max values with a line at the mean ± SD. (**C**) Averaged 30-minute recordings of normalized CBF measured immediately post stroke (0.5hr), 48 hours post PT, and 1 week post PT. Bars represent min to max values with a line at the mean ± SD.

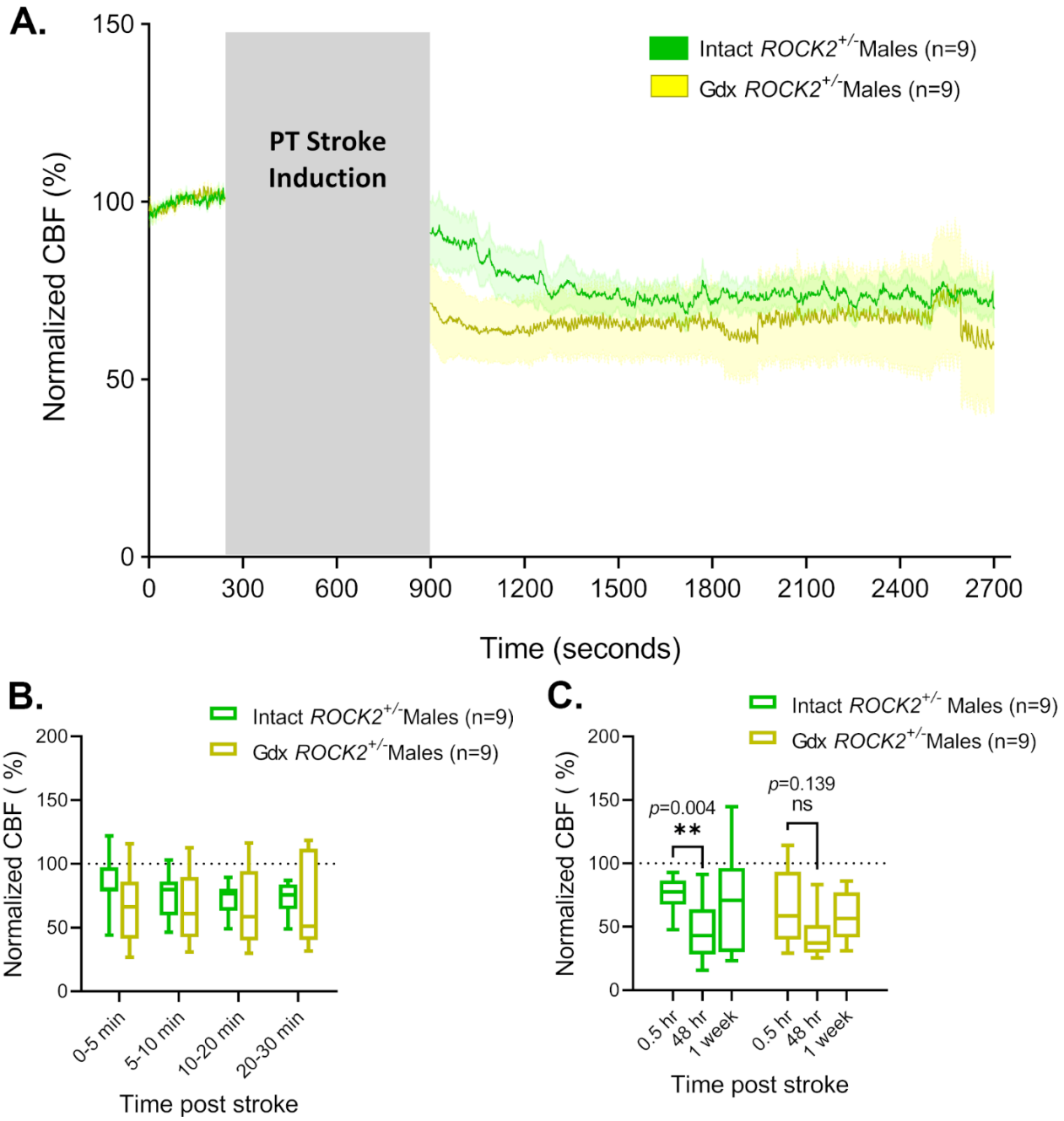

Figure 10. Gonadectomy does not alter the CBF response in *ROCK2*$^{+/-}$ males following PT stroke in the somatosensory cortex.

(**A**) CBF measured by LDF under K/X anesthesia in Intact *ROCK2*$^{+/-}$ male and Gdx *ROCK2*$^{+/-}$ male mice before and after a PT stroke. Grey box indicates time passed during laser irradiation of the PT stroke induction. Post-PT values are normalized to pre-PT baseline values. Curved lines represent average normalized CBF of all animals in the respective group. Shaded area above and below curves represent SEM. (**B**) Averaged CBF measurements of hyperacute timepoints during the 30 minutes immediately following PT stroke induction shown in A. Bars represent min to max values with a line at the mean ± SD. (**C**) Averaged 30-minute recordings of normalized CBF measured immediately post stroke (0.5hr), 48 hours post PT, and 1 week post PT. Bars represent min to max values with a line at the mean ± SD.

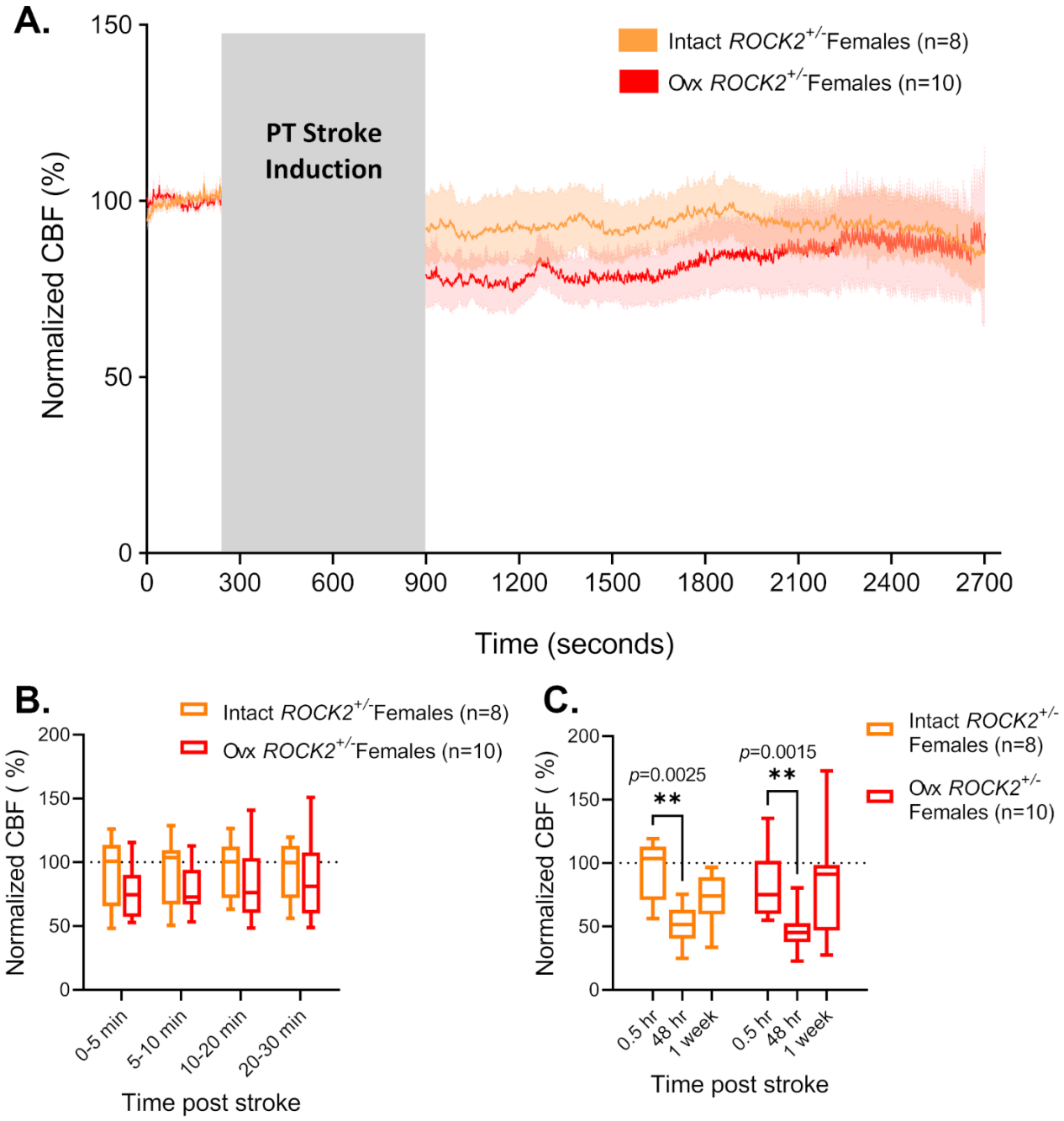

Figure 11. Ovariectomy does not alter the CBF response in *ROCK2*$^{+/-}$ females following PT stroke in the somatosensory cortex.

(**A**) CBF measured by LDF under K/X anesthesia in Intact *ROCK2*$^{+/-}$ female and Ovx *ROCK2*$^{+/-}$ female mice before and after a PT stroke. Grey box indicates time passed during laser irradiation of the PT stroke induction. Post-PT values are normalized to pre-PT baseline values. Curved lines represent average normalized CBF of all animals in the respective group. Shaded area above and below curves represent SEM. (**B**) Averaged CBF measurements of hyperacute timepoints during the 30 minutes immediately following PT stroke induction shown in A. Bars represent min to max values with a line at the mean ± SD. (**C**) Averaged 30-minute recordings of normalized CBF measured immediately post stroke (0.5hr), 48 hours post PT, and 1 week post PT. Bars represent min to max values with a line at the mean ± SD.

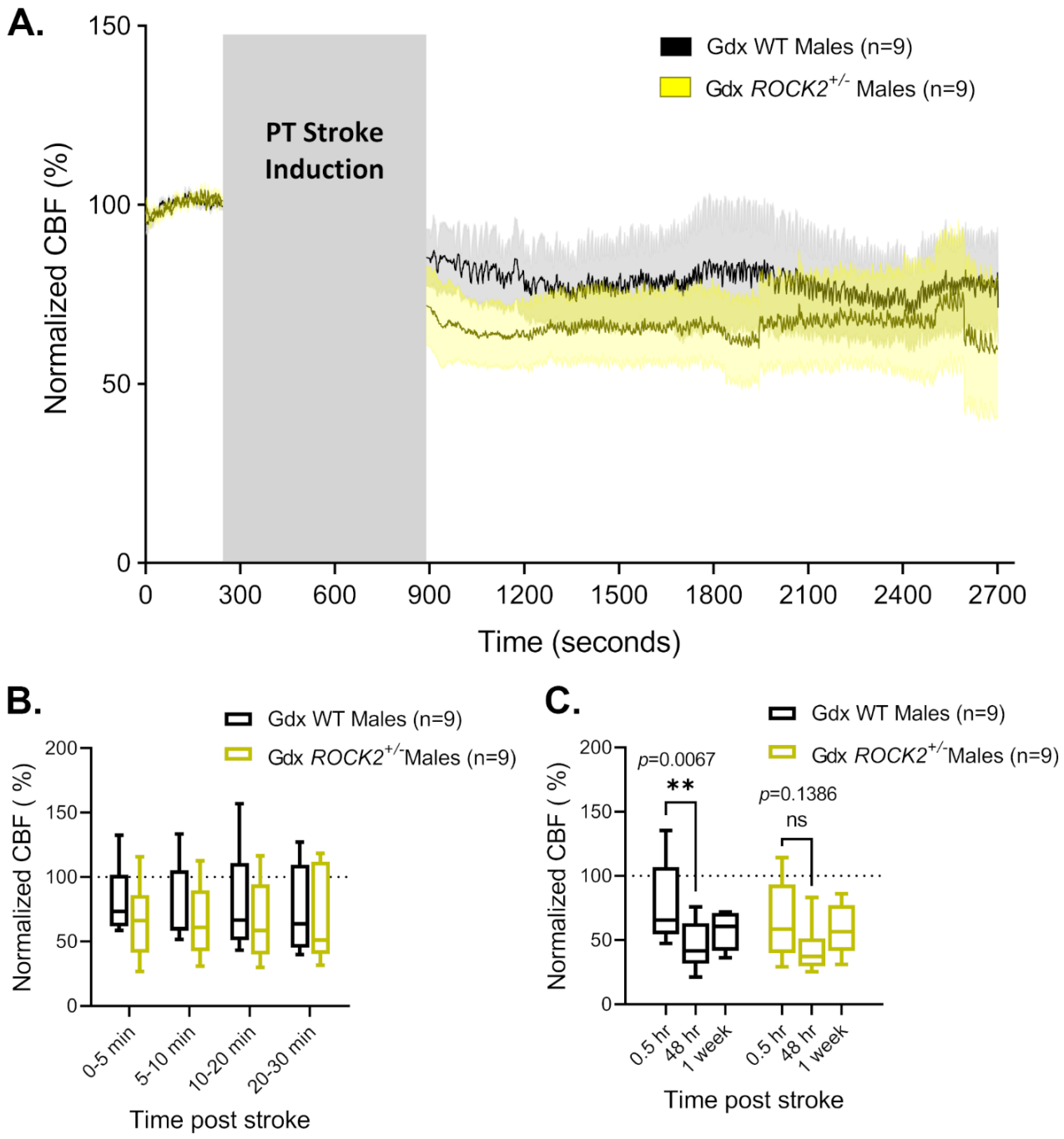

Figure 12. CBF in Gdx WT vs. *ROCK2*$^{+/-}$ males post PT stroke in the somatosensory cortex.

(**A**) CBF measured by LDF under K/X anesthesia in Gdx WT male and Gdx *ROCK2*$^{+/-}$ male mice before and after a PT stroke. Grey box indicates time passed during laser irradiation of the PT stroke induction. Post-PT values are normalized to pre-PT baseline values. Curved lines represent average normalized CBF of all animals in the respective group. Shaded area above and below curves represent SEM. (**B**) Averaged CBF measurements of hyperacute timepoints during the 30 minutes immediately following PT stroke induction shown in A. Bars represent min to max values with a line at the mean ± SD. (**C**) Averaged 30-minute recordings of normalized CBF measured immediately post stroke (0.5hr), 48 hours post PT, and 1 week post PT. Bars represent min to max values with a line at the mean ± SD.

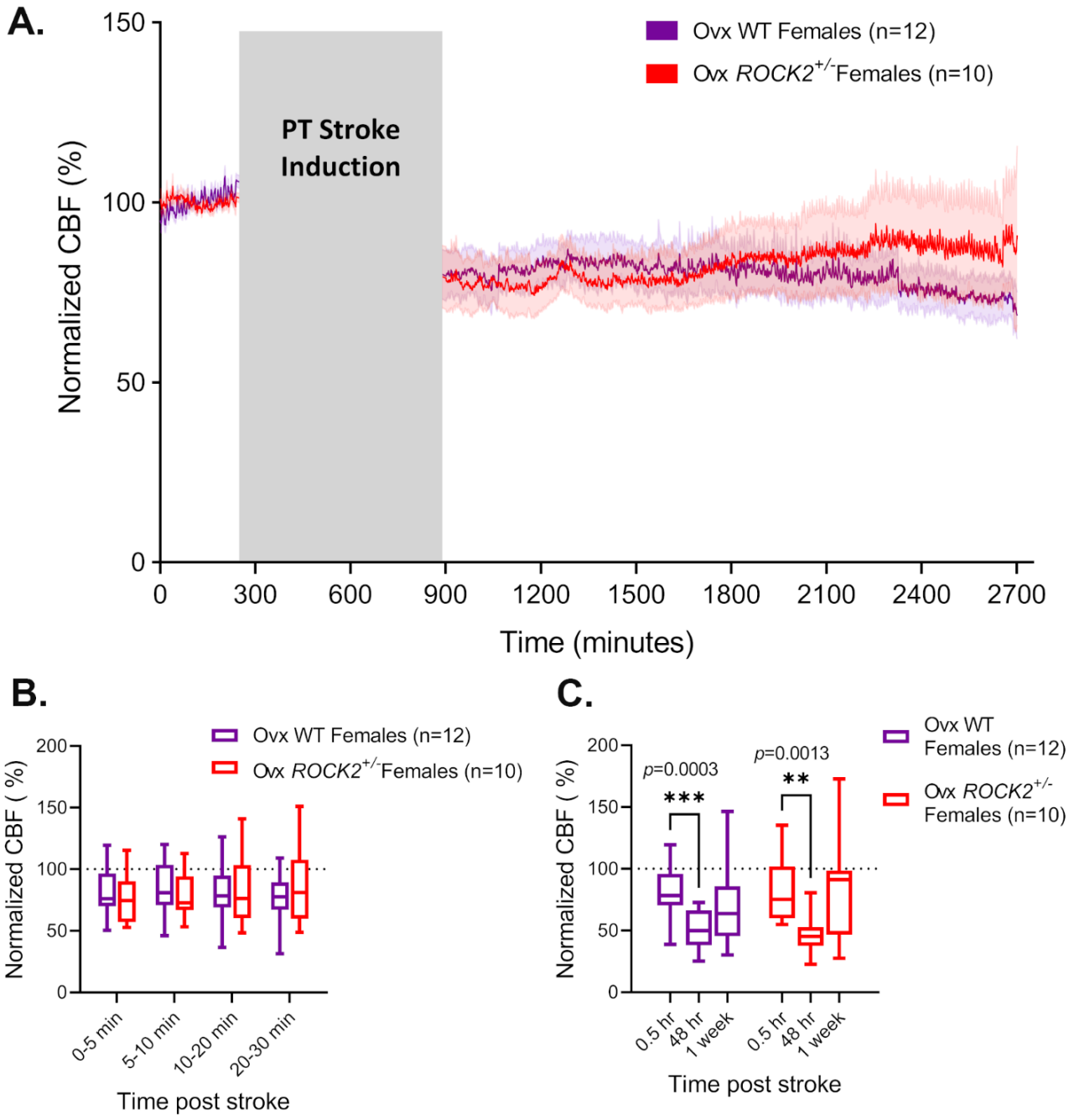

Figure 13. CBF in Ovx WT vs. *ROCK2*$^{+/-}$ females post PT stroke in the somatosensory cortex.

(**A**) CBF measured by LDF under K/X anesthesia in Ovx WT female and Ovx *ROCK2*$^{+/-}$ female mice before and after a PT stroke. Grey box indicates time passed during laser irradiation of the PT stroke induction. Post-PT values are normalized to pre-PT baseline values. Curved lines represent average normalized CBF of all animals in the respective group. Shaded area above and below curves represent SEM. (**B**) Averaged CBF measurements of hyperacute timepoints during the 30 minutes immediately following PT stroke induction shown in A. Bars represent min to max values with a line at the mean ± SD. (**C**) Averaged 30-minute recordings of normalized CBF measured immediately post stroke (0.5hr), 48 hours post PT, and 1 week post PT. Bars represent min to max values with a line at the mean ± SD.

3.5 Infarct Volumes

Infarct volumes were measured 48 hours following PT stroke induction from MRI images. A 2-way ANOVA revealed no significant differences in infarct volumes between any of the groups (**Fig. 14A,B**).

3.6 Nitric Oxide Stain

Staining for nitric oxide was performed using DAF-FM diacetate and DAPI in 2-mm brain sections 24 hours following PT stroke induction. Average intensity of the DAF-FM stain was quantified in the entire infarcted region, determined by the absence of DAPI staining. A 2-way ANOVA revealed no significant differences in average DAF-FM staining intensity between any of the groups (**Fig. 15A,B**).

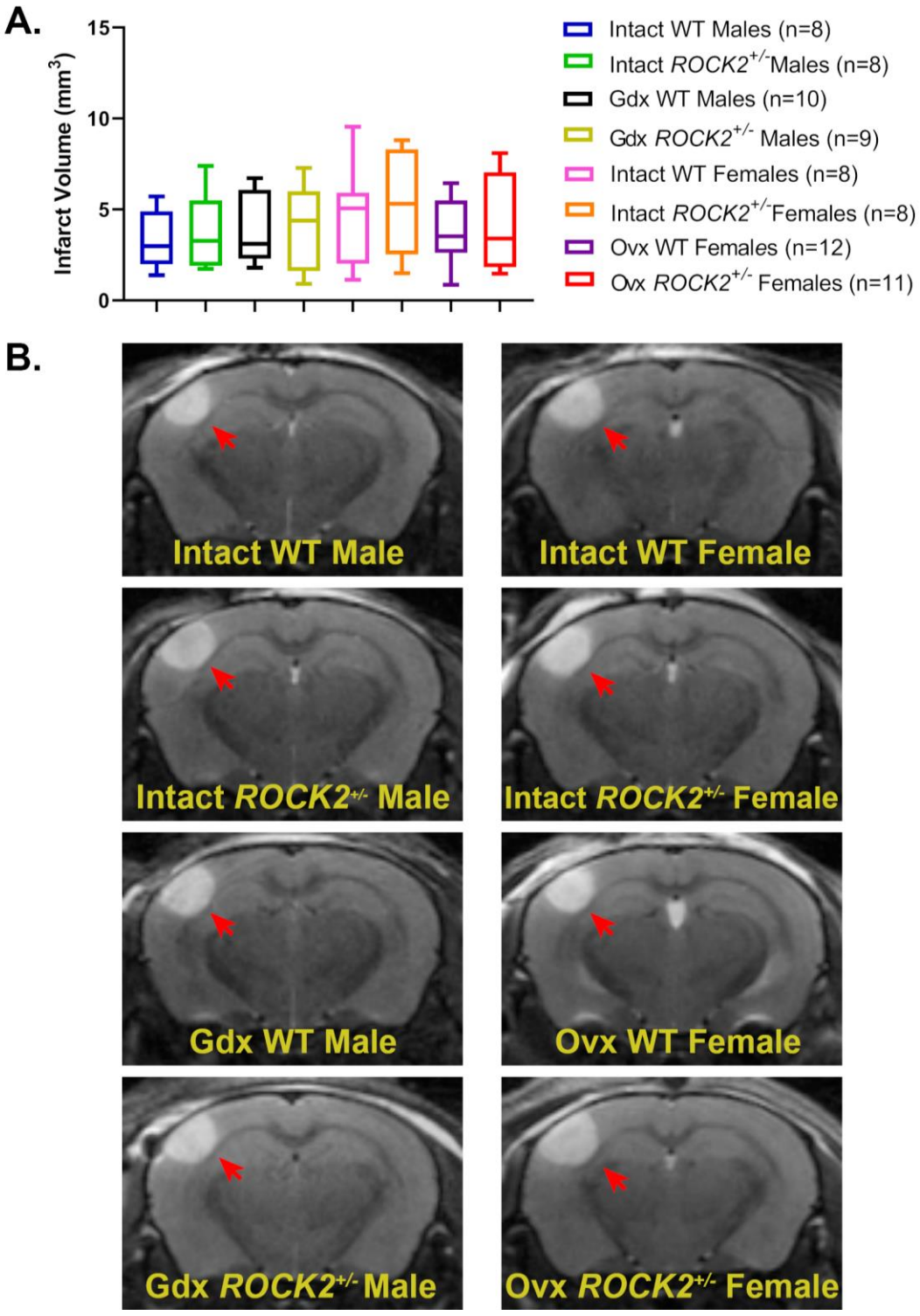

Figure 14. Infarct volume quantification 48 hours following PT stroke.

(**A**) Quantification of total infarct volumes measured from magnetic resonance imaging (MRI) images taken 48 hours following PT stroke induction in the somatosensory cortex. Bars represent min to max points with a line at the mean ± SD. (**B**) Representative MRI images of infarcts at 48 hours post PT stroke. Red arrows point to infarct lesion.

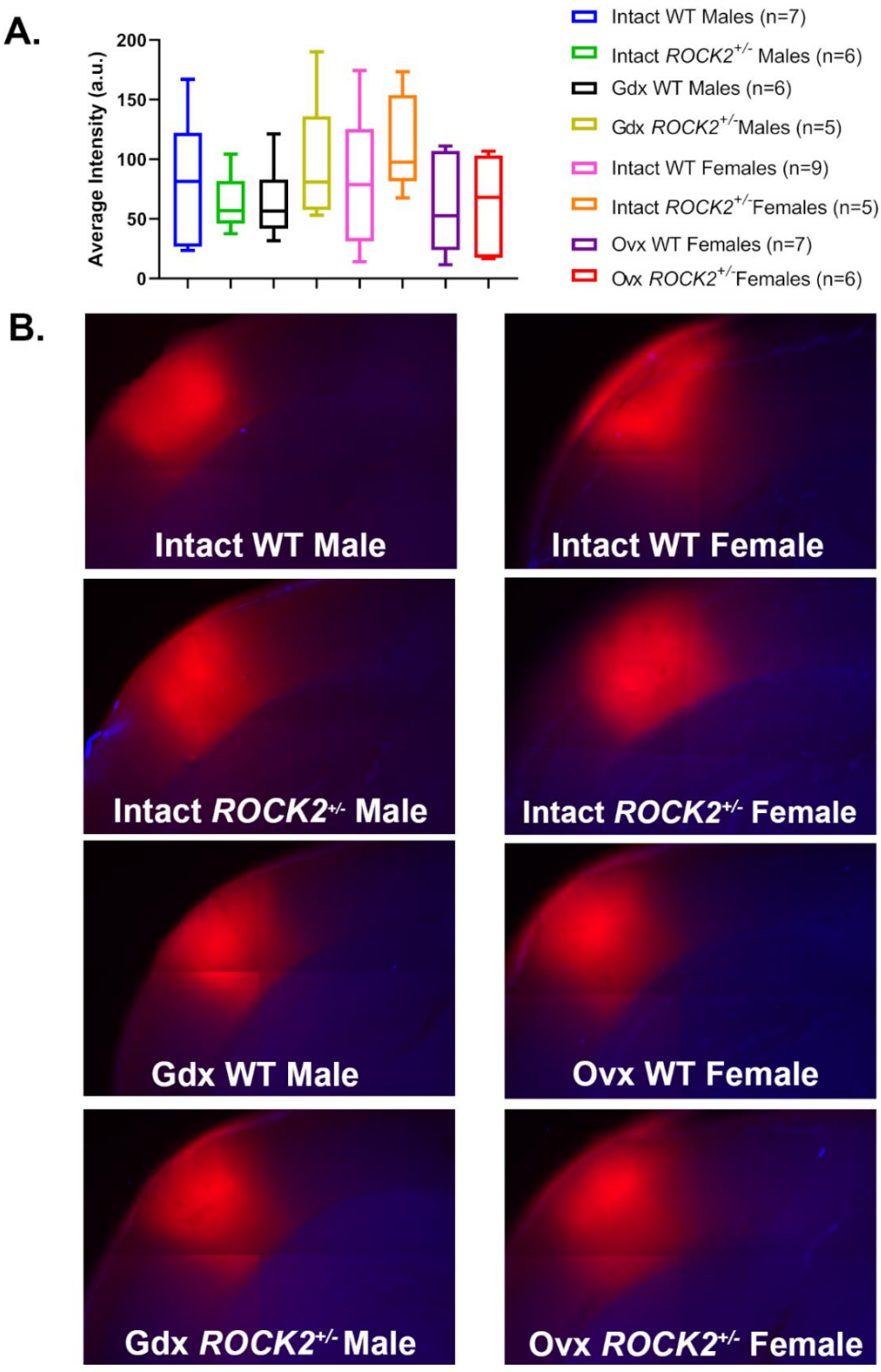

Figure 15. Nitric oxide staining in the infarct 24 hours following PT stroke.

(**A**) Quantification of average intensity encompassing entire infarct after staining with DAF-FM diacetate staining performed 24 hours following PT stroke induction in the somatosensory cortex. Bars represent min to max points with a line at the mean ± SD. (**B**) Representative images of brain slices stained with DAF-FM diacetate (red) and DAPI (blue).

4. Discussion

The current project investigated CBF outcomes following PT stroke using LDF to provide high temporal resolution of the CBF response. CBF was characterized immediately following stroke and up to one week following stroke in intact and gonadectomized male and female *ROCK2*$^{+/-}$ mice. This study provides novel insight into the mechanisms involved in sex differences in CBF values following stroke in a preclinical stroke mode. Overall, there is a marked difference between males and females in the acute CBF responses to PT stroke, which appears to be mediated by endogenous female sex hormones and rho-kinase.

4.1 CBF Outcomes in Intact Wild-type Males and Females Following PT Stroke

The CBF response in Intact WT males displayed a phenotypic delayed drop in CBF in the immediate 30-minute timepoint post-stroke compared to Intact WT females. Intact WT males also show a further reduction in CBF at the 48-hour timepoint post stroke, whereas Intact WT females show no change at this timepoint. This apparent sex difference may be due to several factors, including differences in the way each sex responds to stroke induction for this particular stroke model. PT stroke induction involves initiation of the coagulation cascade, resulting in thrombus formation. In both animal models and human studies, females have higher levels of platelets in circulation, and furthermore, platelets from females display higher reactivity and are more prone to aggregation and thrombus formation (Zwierzina, et al., 1987; Green, et al., 1992; Leng, et al., 2004; Becker, et al., 2006; Otahbachi, et al., 2010; Miller, et al., 2014; Friede, et al., 2020). Because Intact WT males appear to take longer to reach maximal CBF deficit – exhibiting peak CBF drop when measured 48 hours following stroke induction – it is possible that PT stroke induction may require more time for platelet aggregation to occur, resulting in the

observed delay in CBF drop. Indeed, evidence that female platelets are more reactive and prone to thrombosis supports the idea that thrombus formation resulting from PT stroke induction may have a quicker onset in the female sex.

The only study to directly compare CBF between males and females following ischemic stroke showed that after 2 hours of transient intraluminal MCAo, intact female rats had higher CBF values measured by LDF under halothane anesthesia compared to both intact males as well as Ovx females (Alkayed, et al., 1998). This improvement in CBF deficit also corresponded to decreased infarct volumes in intact females. There were no improvements at any timepoint post stroke in CBF values in females in the current study, which may be due to mechanistic properties of the stroke model used. Transient MCAo induces ischemic stroke in a much different way than PT stroke, involving ligation of the MCA for a pre-determined amount of time followed by rapid reperfusion, and can involve a secondary injury called reperfusion injury. The PT stroke model does not involve any reperfusion, only that which occurs by endogenous fibrinolysis of the thrombotic clot, which results in a much slower and incomplete reperfusion of the affected tissue. Therefore, measuring CBF following MCAo is also assessing the response to reperfusion injury and is a measure of neuroprotection, not just occlusion of the vessel. While females appear to be protected in stroke models involving rapid reperfusion, this may not be the case for the PT stroke model.

4.2 Contribution of Endogenous Sex Hormones to CBF Outcomes Following PT Stroke

Endogenous male sex hormones were removed by gonadectomy of WT males a minimum of 10 days prior to inducing PT stroke and measuring CBF values. There were no differences in the hyperacute phase post stroke of CBF values in Gdx WT males when compared

to Intact WT males. Similarly, Gdx WT males showed the same delay in reaching maximal CBF drop post PT as Intact WT males. This suggests that removing endogenous male sex hormones does not alter CBF outcomes following a PT stroke in the somatosensory cortex.

Endogenous female sex hormones were removed by bilateral ovariectomy of WT females a minimum of 10 days prior to PT stroke induction. Interestingly, Ovx of WT females produced a similar phenotype as was observed in both Intact and Gdx WT males. Although not statistically significant, there is a clear separation between the curves of Ovx WT females and Intact WT females in the 0-5 minute hyperacute phase following stroke, where Ovx WT females have slightly higher CBF values immediately following stroke, showing the same phenotype as seen in both aforementioned male groups. Moreover, Ovx WT females also show a delayed drop in CBF, reaching a maximal drop in CBF when measured 48 hours following stroke. These results suggest that endogenous female sex hormones may be involved in the thrombotic response of PT stroke induction. Indeed, chronic E2 treatment exacerbated platelet aggregation in response to endothelial injury of cerebral microvessels in both male and female mice (Rosenblum, et al., 1985). Conversely, chronic testosterone or DHT treatment of male mice increased platelet aggregation following endothelial injury to mesenteric arteries, but not cerebral pial vessels, and furthermore, had no effect on aggregation in female mice (Rosenblum, et al., 1987). Therefore, it is possible that removing endogenous estrogens from female mice through Ovx results in less platelet aggregation and thrombus formation during PT stroke induction, producing this delayed drop in CBF and the same phenotypic response that was observed in males.

4.3 Rho-kinase modulates the CBF response to PT stroke in a sex-specific manner

CBF outcomes were not different at any timepoint in intact males between WT and *ROCK2*$^{+/-}$ genotypes, suggesting the ROCK2 haploinsufficiency does not alter the CBF response to stroke in males. While ROCK deletion and inhibition has been shown to be neuroprotective against tissue damage and behavioural outcomes of ischemic stroke, there are somewhat conflicting results in terms of the role of ROCK in CBF outcomes following stroke in preclinical models. Male mice treated with the non-selective ROCK inhibitor fasudil, had increased CBF values at baseline compared to control mice, however there were no differences in regional CBF between groups following transient MCAo (Rikitake, et al., 2005). Alternatively, non-selective ROCK inhibition did attenuate the CBF deficit in mice subjected to distal MCAo, but not in mice lacking the gene for eNOS (*eNOS*$^{-/-}$), suggesting an endothelial-dependent mechanism of neuroprotection (Shin, et al., 2007). On the other hand, selective inhibition of the ROCK2 isoform with KD025 did not improve absolute CBF values of male mice following distal MCAo, but did reduce the overall area of tissue with a severe perfusion deficit (Lee, et al., 2014). Finally, heterozygous knockout of ROCK2, but not ROCK1, in male mice improved absolute CBF following 1-hour of transient MCAo as measured by an indicator fractionation technique (Hiroi, et al., 2018). While there is some evidence that ROCK inhibition and deletion improves CBF outcomes following stroke, this was not observed in the current study. This may be due to the nature of the stroke model used, wherein PT stroke does not provide reperfusion injury and is less sensitive to measurements of neuroprotection. A failure to detect CBF improvement could also be due to the measuring technique used. In studies that do show some improvement in CBF following stroke, the techniques used offer a larger picture of total CBF deficit in the entire brain, whereas LDF provides high temporal resolution of only a very small area surrounding the

infarct core. It is possible that there may have been CBF improvements in *ROCK2*$^{+/-}$ mice in the current study as has been previously described in other studies (Lee, et al., 2014; Hiroi, et al., 2018), but it simply could not be detected with the LDF method used.

Haploinsufficiency for the ROCK2 gene in intact female mice demonstrated profound differences in CBF values following PT stroke. Compared to Intact WT females, Intact *ROCK2*$^{+/-}$ females had significantly higher CBF values in the immediate 30-minute time period following stroke. Additionally, Intact *ROCK2*$^{+/-}$ females showed the same delayed drop in CBF values that was observed in both groups of intact males, as well as in Ovx WT females, wherein the maximal drop in CBF was observed at 48 hours following stroke. This sex-specific role of ROCK2 in CBF outcomes may be due to differences in RhoA/ROCK signaling in platelets, which has been shown to be upregulated in platelets from females and contributes to platelet hyperreactivity in females (Schubert, et al., 2016). It is possible that increased RhoA/ROCK signaling in platelets makes them more reactive to thrombus formation during PT stroke induction, therefore reducing the amount of ROCK2 available in hyperreactive female platelets could increase the necessary time for thrombosis to occur, resulting in the phenotypic male CBF response observed in this particular model. Indeed, platelets from male mice that harbor a ROCK2 deletion selectively in platelets were less prone to aggregation and thrombosis, and also had improved CBF following a thromboembolic model of MCAo compared to WT mice (Sladojevic, et al., 2017).

4.4 Interactions Between Sex Hormones and ROCK2 in CBF Outcomes Following PT Stroke

Contrary to comparisons made between males and females in intact WT mice, there were no differences in the behaviour of CBF at any timepoint post stroke between sexes in intact

ROCK2$^{+/-}$ mice. Removal of endogenous sex hormones from *ROCK2*$^{+/-}$ males and females also did not alter the CBF response at any timepoint post stroke. Overall, regardless of genotype or gonadectomy status, male mice showed a phenotypic response in CBF following stroke where they do not reach a maximal drop in CBF that is expected with stroke until 48 hours following stroke induction. Although not statistically significant from the measurements taken immediately post stroke, Gdx *ROCK2*$^{+/-}$ males still displayed peak drop in CBF values when measured at 48 hours following stroke induction. Meanwhile, removal of endogenous sex hormones from WT females produced the same phenotype as observed in males. Lastly, *ROCK2*$^{+/-}$ females also showed the phenotypic response of delayed CBF drop, which was unaffected by removing endogenous sex hormones.

Given the potential for estrogen to upregulate RhoA/ROCK signaling, it is possible that removing endogenous estrogens downregulates ROCK and therefore reduces its activity in platelets, reducing thrombus formation in this particular model of ischemic stroke. Indeed, as described earlier, estrogen treatment may also contribute to increased reactivity and aggregation of platelets. Therefore, decreased estrogen may alter RhoA/ROCK signaling in platelets, contributing to a decrease in their reactivity and potentially delaying aggregation and thrombus formation during PT stroke induction.

4.5 Infarct Volumes and Nitric Oxide Staining

There were no differences in stroke lesion volumes as determined by MRI measured 48 hours following stroke induction. Although previous studies have reported a neuroprotective role of ROCK inhibition or deletion in ischemic stroke and infarct volume reduction, these were all reported using variations of the MCAo model. While MCAo is useful for characterizing

neuroprotection, the model produces quite large strokes in which up to half of the affected hemisphere is lesioned, which has been argued to not be representative of clinical strokes seen in humans (Carmichael, 2005). This study is the first to characterize ROCK2 deletion in a small, focal ischemic stroke, that may better mimic clinical conditions. Importantly, because there were no differences in infarct volume between groups, it confirms that differences observed in CBF measurements are not due to a larger area of injury which correlates with a more severe CBF deficit.

ROCK negatively regulates eNOS function, providing speculation that the neuroprotective role of ROCK inhibition and deletion is mediated through upregulation of eNOS. Given the evidence that *ROCK2*$^{+/-}$ mice have increased eNOS levels in brain ECs (Hiroi, et al., 2018) we assessed levels of NO in the infarct 24 hours following PT stroke induction using DAF-FM diacetate staining. There were no differences in NO levels in any group following PT stroke, despite a previous study using the same stain showing increased NO levels at the same timepoint following transient MCAo in *ROCK2*$^{+/-}$ male mice compared to both *ROCK1*$^{+/-}$ and WT mice (Hiroi, et al., 2018). Again, this may be due to differences in mechanisms of ischemic stroke models. Unlike MCAo, the PT stroke model does not have any reperfusion injury, so eNOS upregulation may be more prevalent in stroke models with reperfusion. If this were true, haploinsufficiency of ROCK2 would reduce eNOS inhibition resulting in increased NO bioavailability following MCAo. Additionally, NO has an extremely short half life and staining may not have been done quickly enough to detect any differences. Further experiments such as eNOS and ROCK activity assays would be required to solidify the absence of eNOS upregulation in *ROCK2*$^{+/-}$ mice following PT stroke in the somatosensory cortex.

4.6 Limitations and Future Directions

To support the hypothesis that Intact WT females have a more severe reduction in CBF following PT stroke due to accelerated thrombosis, further experimentation would be required to support this. Performing a coagulation assay would first be necessary to assess if Intact WT females are more prone to blood coagulation than other groups. From there, assessing platelet reactivity and also determining ROCK activity in platelets in these groups would further elucidate the precise mechanisms involved. It would also be interesting to assess eNOS activity and ROCK activity in brain ECs to determine if these are upregulated following PT stroke, as most studies characterizing these have been performed using MCAo.

Additionally, all CBF measurements were performed under K/X anesthesia. This anesthesia was chosen because it has lesser effects on vasodilation than other vaporized anesthetics such as isoflurane (Rakymzhan, et al., 2021), which also has neuroprotective properties against ischemic stroke via modulation of eNOS (Kehl, et al., 2002; Krolikowski, et al., 2006; Lu, et al., 2017). However, there is still evidence that ketamine can cause vasodilation and alter CBF (Rakymzhan, et al., 2021). Ideally, these experiments would be repeated in awake and unanesthetized mice, which has been successfully performed with PT stroke using cranial window preparations in rats (Lu, et al., 2014; Yang, et al., 2019) and mice (He, et al., 2020). This would better mimic clinical stroke conditions and eliminate any confounding effects of anesthetics.

4.7 Conclusion

Overall, there is a clear sex difference in CBF outcomes following stroke in this model of PT stroke in the somatosensory cortex, in which ROCK2 appears to be implicated. All groups

except for Intact WT females show a delayed drop in CBF values, reaching a maximal drop in CBF at 48 hours following stroke induction. This is likely due to mechanistic differences in stroke induction, where both ROCK2 and endogenous female sex hormones, most likely estrogen, mediate platelet aggregation and thrombus formation resulting in delayed obstruction of the vessels in the infarct. Sex differences in response to different stroke models reiterates the importance of studying both sexes in the pathogenesis of disease. Characterization of stroke models in both males and females is of the utmost importance in preclinical research to prevent translational failure. This research helps clarify the role of ROCK2 in CBF outcomes following a PT stroke, and brings to light new questions about interactions between rho-kinase and sex hormones in the cerebrovasculature.

References

Abd-Elrahman, K. S., Walsh, M. P. & Cole, W. C., 2015. Abnormal Rho-associated kinase activity contributes to the dysfunctional myogenic response of cerebral arteries in type 2 diabetes. *Canadian Journal of Physiology and Pharmacology,* 93(3), pp. 177-184.

Ahnstedt, H. et al., 2013. Male-female differences in upregulation of vasoconstrictor responses in human cerebral arteries. *PloS one,* 8(4), p. e62698.

Ahnstedt, H., McCullough, L. D. & Cipolla, M. J., 2016. The Importance of Considering Sex Differences in Translational Stroke Research. *Transl Stroke Res,* Volume 7, pp. 261-273.

Alkayed, N. J. et al., 1998. Gender-linked brain injury in experimental stroke. *Stroke,* Volume 29, pp. 159-165.

Allen, C., Srivastava, K. & Bayraktutan, U., 2010. Small GTPase RhoA and its effector Rho-kinase mediate oxygen glucose deprivation-evoked in vitro cerebral barrier dysfunction. *Stroke,* Volume 41, p. 2056–2063.

Amin-Hanjani, S. et al., 2001. Mevastatin, an HMG-CoA reductase inhibitor, reduces stroke damage and upregulates endothelial nitric oxide synthase in mice. *Stroke,* 32(4), pp. 980-986.

Andreone, B. J., Lacoste, B. & Gu, C., 2015. Neuronal and vascular interactions. *Annu Rev Neurosci,* Volume 38, pp. 24-46.

Appelros, P., Stegmayr, B. & Terent, A., 2009. Sex differences in stroke epidemiology: a systematic review. *Stroke,* Volume 40, pp. 1082-1090.

Attwell, D. A. & Laughlin, S., 2001. An Energy Budget for Signaling in the Grey Matter of the Brain. *Journal of Cerebral Blood Flow and Metabolism,* Volume 21, pp. 1133-1145.

Attwell, D. et al., 2010. Glial and neuronal control of brain blood flow. *Nature,* Volume 468, pp. 232-243.

Azad, N., Pitale, S., Barnes, W. E. & Friedman, N., 2003. Testosterone treatment enhances regional brain perfusion in hypogonadal men. *The Journal of Clinical Endocrinology & Metabolism,* 88(7), pp. 3064-3068.

Barker-Collo, S. et al., 2015. Sex Differences in Stroke Incidence, Prevalence, Mortality and Disability-Adjusted Life Years: Results from the Global Burden of Disease Study 2013. *Neuroepidemiology,* Volume 45, pp. 203-214.

Becker, D. M. et al., 2006. Sex differences in platelet reactivity and response to low-dose aspirin therapy. *JAMA,* 295(12), pp. 1420-1427.

Ben-Zvi, A. et al., 2014. Mfsd2a is critical for the formation and function of the blood-brain barrier. *Nature,* Volume 509, pp. 507-511.

Blakemore, J. & Naftolin, F., 2016. Aromatase: Contributions to Physiology and Disease in Women and Men. *PHYSIOLOGY,* Volume 31, p. 258–269.

Boese, A. C. et al., 2017. Sex differences in vascular physiology and pathophysiology: Estrogen and androgen signaling in health and disease. *Am J Physiol Heart Circ Physiol,* Volume 313, p. H524–H545.

Bonkhoff, A. K. et al., 2021. Outcome after acute ischemic stroke is linked to sex-specific lesion patterns. *Nat Commun 12, 3289 (2021),* Volume 12, pp. 1-14.

Brouns, R. & De Deyn, P. P., 2009. The complexity of neurobiological processes in acute ischemic stroke. *Clinical Neurology and Neurosurgery,* Volume 111, pp. 483-495.

Brown, K. F. et al., 2018. The fraction of cancer attributable to modifiable risk factors in England, Wales, Scotland, Northern Ireland, and the United Kingdom in 2015. *Br J Cancer,* Volume 118, pp. 1130-1141.

Bushnell, C. D. et al., 2018. Sex differences in stroke: Challenges and opportunities. *Journal of Cerebral Blood Flow and Metabolism,* 38(12), p. 2179–2191.

Carmichael, S. T., 2005. Rodent models of focal stroke: size, mechanism, and purpose. *NeuroRx,* Volume 2, pp. 396-409.

Cauli, B. & Hamel, E., 2010. Revisiting the role of neurons in neurovascular coupling. *Front Neuroenergetics,* Volume 2, pp. 1-8.

Chen, J. et al., 2002. VEGF-induced mobilization of caveolae and increase in permeability of endothelial cells. *Am J Physiol Cell Physiol,* Volume 282, pp. C1053-1063.

Chen, K., Pittman, R. N. & Popel, A. S., 2008. Nitric oxide in the vasculature: where does it come from and where does it go? A quantitative perspective. *Antioxidants & Redox Signaling,* 10(7), pp. 1185-1198.

Chrissobolis, S., Budzyn, K., Marley, P. D. & Sobey, C. G., 2004. Evidence that estrogen suppresses rho-kinase function in the cerebral circulation in vivo. *Stroke,* 35(9), pp. 2200-2205.

Çiçek, F. & Ayaz, M., 2015. The Isoform Spesific Roles of Rho-Kinases in Vascular Diseases. *Journal of Cardiol Ther,* 2(6), pp. 465-468.

Cosgrove, K. P., Mazure, C. M. & Staley, J. K., 2007. Evolving knowledge of sex differences in brain structure, function, and chemistry. *Biol Psychiatry,* Volume 62, pp. 847-855.

Cowan, R. L. et al., 2017. Sex Differences in the Psychophysical Response to Contact Heat in Moderate Cognitive Impairment Alzheimer's Disease: A Cross-Sectional Brief Report. *J Alzheimers Dis,* Volume 60, pp. 1633-1640.

Cui, Q., Zhang, Y., Chen, H. & Li, J., 2013. Rho kinase: A new target for treatment of cerebral ischemia/reperfusion injury.. *Neural Regen Res,* Volume 8, pp. 1180-1189.

Daneman, R., 2012. The blood-brain barrier in health and disease. *Ann Neurol,* Volume 72, pp. 648-672.

De Silva, T. M. et al., 2016. Heterogeneous Impact of ROCK2 on Carotid and Cerebrovascular Function. *Hypertension,* Volume 68, pp. 809-817.

Deb, P., Sharma, S. & Hassan, K. M., 2010. Pathophysiologic mechanisms of acute ischemic stroke: An overview with emphasis on therapeutic significance beyond thrombolysis. *Pathophysiology,* 17(3), pp. 197-218.

Faraci, F. M. et al., 2006. Cerebral vascular effects of angiotensin II: new insights from genetic models. *J Cereb Blood Flow Metab,* 26(4), pp. 449-455.

Feng, Y. et al., 1999. VEGF-induced permeability increase is mediated by caveolae. *Invest Ophthalmol Vis Sci,* Volume 40, pp. 157-167.

Fisher, M., 2008. Injuries to the vascular endothelium: Vascular wall and endothelial dysfunction. *Rev Neurol Dis,* Volume 5 Suppl 1, pp. S4-11.

Fleming, I., 2010. Molecular mechanisms underlying the activation of eNOS. *Eur J Physiol,* Volume 459, pp. 793-806.

Fredriksson, I., Fors, C. & Johansson, J., 2007. Laser doppler flowmetry: A theoretical framework. *Department of Biomedical Engineering, Linköping University,* pp. 1-22.

Freitas-Andrade, M., Raman-Nair, J. & Lacoste, B., 2020. Structural and Functional Remodeling of the Brain Vasculature Following Stroke. *Frontiers in Physiology,* 11(948), pp. 1-28.

Friede, K. A. et al., 2020. Influence of Sex on Platelet Reactivity in Response to Aspirin. *J Am Heart Assoc,* 9(14), p. e014726..

Fujii, B. et al., 2012. Inhibition of Rho kinase by hydroxyfasudil attenuates brain edema after subarachnoid hemorrhage in rats. *Neurochem Int,* Volume 60, pp. 327-333.

Fukuda, K. et al., 2000. Ovariectomy exacerbates and estrogen replacement attenuates photothrombotic focal ischemic brain injury in rats. *Stroke,* Volume 31, pp. 155-159.

Fu, Z. et al., 2014. Increased activity of Rho kinase contributes to hemoglobin-induced early disruption of the blood-brain barrier in vivo after the occurrence of intracerebral hemorrhage. *Int J Clin Exp Pathol,* Volume 7, pp. 7844-7853.

Ghisleni, C. et al., 2015. Effects of Steroid Hormones on Sex Differences in Cerebral Perfusion. *PLoS ONE,* 10(9), pp. 1-15.

Gibson, C. L. et al., 2014. Inhibition of Rho-kinase protects cerebral barrier from ischaemia-evoked injury through modulations of endothelial cell oxidative stress and tight junctions. *J Neurochem,* 129(5), pp. 816-826.

Girouard, H. & Iadecola, C., 2006. Neurovascular coupling in the normal brain and in hypertension, stroke, and Alzheimer disease. *Journal of Applied Physiology,* Volume 100, p. 328 –335.

Goyal, M. et al., 2015. Randomized Assessment of Rapid Endovascular Treatment of Ischemic Stroke. *The New England Journal of Medicine,* Volume 372, pp. 1019-1030.

Green, M. S., Peled, I. & Najenson, T., 1992. Gender differences in platelet count and its association with cigarette smoking in a large cohort in Israel. *J Clin Epidemiol,* 45(1), pp. 77-84.

Guo, J. et al., 2010. Estrogen-receptor-mediated protection of cerebral endothelial cell viability and mitochondrial function after ischemic insult in vitro. *J Cereb Blood Flow Metab,* Volume 30, pp. 545-554.

Gurewich, V., 2016. Thrombolysis: A Critical First-Line Therapy with an Unfulfilled Potential. *Am J Med,* Volume 129, pp. 573-575.

Hacke, W. et al., 2008. Thrombolysis with alteplase 3 to 4.5 hours after acute ischemic stroke. *New England Journal of Medicine,* Volume 359, pp. 17-29.

Hale, G. E. & Shufelt , C. L., 2015. Hormone therapy in menopause: An update on cardiovascular disease considerations. *Trends Cardiovasc Med,* Volume 25, pp. 540-549.

Haley, M. J. & Lawrence, C. B., 2017. The blood-brain barrier after stroke: Structural studies and the role of transcytotic vesicles. *J Cereb Blood Flow Metab,* 37(2), pp. 456-470.

Hao, Z. et al., 2016. Atorvastatin Plus Metformin Confer Additive Benefits on Subjects with Dyslipidemia and Overweight/Obese via Reducing ROCK2 Concentration. *Exp Clin Endocrinol Diabetes,* Volume 124, pp. 246-250.

Hartmann, S., Ridley, A. J. & Lutz, S., 2015. The function of Rho-associated kinases ROCK1 and ROCK2 in the pathogenesis of cardiovascular disease. *Frontiers in Pharmacology,* Volume 6, pp. 1-16.

Heart & Stroke Foundation of Canada, 2019. (Dis)connected: How unseen links are putting us at risk. *Heart and Stroke Report,* pp. 1-24.

Hebert, M., Lesept, F., Vivien, D. & Macrez, R., 2016. The story of an exceptional serine protease, tissue-type plasminogen activator (tPA). *Rev Neurol,* Volume 172, pp. 186-197.

He, F. et al., 2020. Multimodal mapping of neural activity and cerebral blood flow reveals long-lasting neurovascular dissociations after small-scale strokes. *Sci Adv,* 6(21), pp. 1-12.

He, F. et al., 2020. Multimodal mapping of neural activity and cerebral blood flow reveals long-lasting neurovascular dissociations after small-scale strokes. *Science Advances,* Volume 6, p. eaba1933.

Heiss, W. D., 2012. The ischemic penumbra: How does tissue injury evolve?. *Annals of the New York Academy of Sciences,* Volume 1268, pp. 26-34.

Hendrix, S. L. et al., 2006. Effects of conjugated equine estrogen on stroke in the Women's Health Initiative. *Circulation,* Volume 113, pp. 2425-2434.

Hillman, E. M., 2014. Coupling mechanism and significance of the BOLD signal: a status report. *Annu Rev Neurosci,* Volume 37, pp. 161-181.

Hiroi, Y. et al., 2018. Neuroprotection Mediated by Upregulation of Endothelial Nitric Oxide Synthase in Rho-Associated, Coiled-Coil-Containing Kinase 2 Deficient Mice. *Circulation.*

Hofer, A. et al., 2007. Sex differences in brain activation patterns during processing of positively and negatively valenced emotional words. *Psychological Medicine,* 37(1), pp. 109-119.

Hossmann, K. A., 2012. The two pathophysiologies of focal brain ischemia: implications for translational stroke research. *J Cereb Blood Flow Metab,* 32(7), pp. 1010-16.

Howarth, C., 2014. The contribution of astrocytes to the regulation of cerebral blood flow. *Frontiers in Neuroscience,* Volume 8, p. 103.

Iadecola, C. & Anrather, J., 2011. The immunology of stroke: from mechanisms to translation. *Nature Medicine,* 17(7), pp. 796-808.

Jauch, E. C. et al., 2013. Guidelines for the early management of patients with acute ischemic stroke: A guideline for healthcare professionals from the American Heart Association/American Stroke Association. *Stroke,* Volume 44, pp. 870-947.

Jin, H. G. et al., 2006. Hypoxia-induced upregulation of endothelial small G protein RhoA and Rho-kinase/ROCK2 inhibits eNOS expression. *Neuroscience Letters,* Volume 408, p. 62–67.

Ju, H., Zou, R., Venema, V. J. & Venema, R. C., 1997. Direct interaction of endothelial nitric-oxide synthase and caveolin-1 inhibits synthase activity. *J Biol Chem,* Volume 272, pp. 18522-18525.

Kehl, F. et al., 2002. Isoflurane-induced cerebral hyperemia is partially mediated by nitric oxide and epoxyeicosatrienoic acids in mice in vivo. *Anesthesiology,* 97(6), pp. 1528-1533.

Knowland, D. et al., 2014. Stepwise recruitment of transcellular and paracellular pathways underlies blood-brain barrier breakdown in stroke. *Neuron,* Volume 82, pp. 603-617.

Kowalczyk, A. et al., 2015. The role of endothelin-1 and endothelin receptor antagonists in inflammatory response and sepsis. *Arch Immunol Ther Exp,* 63(1), p. 41–52.

Krause, D. N., Duckles, S. P. & Pelligrino, D. A., 2006. Influence of sex steroid hormones on cerebrovascular function. *J Appl Physiol,* Volume 101, pp. 1252-1261.

Krolikowski, J. G. et al., 2006. Role of Erk1/2, p70s6K, and eNOS in isoflurane-induced cardioprotection during early reperfusion in vivo. *Can J Anaesth,* 53(2), pp. 174-182.

Krueger, H. et al., 2015. Prevalence of Individuals Experiencing the Effects of Stroke in Canada. *Stroke,* 46(8), pp. 2226-2231.

Lacoste, B. & Gu, C., 2015. Control of cerebrovascular patterning by neural activity during postnatal development. *Mech Dev,* Volume 138, pp. 43-49.

Lamping, K. G. & Faraci, F. M., 2001. Role of sex differences and effects of endothelial NO synthase deficiency in responses of carotid arteries to serotonin. *Arterioscler Thromb Vasc Biol,* Volume 21, p. 523–528.

Laufs, U. & Liao, J. K., 1998. Post-transcriptional regulation of endothelial nitric oxide synthase mRNA stability by Rho GTPase. *J Biol Chem,* 273(37), p. 24266–24271.

Lecrux, C. & Hamel, E., 2011. The neurovascular unit in brain function and disease. *Acta Physiol,* 203(1), pp. 47-59.

Lee, J. et al., 2014. Lee, J., Zheng, Y., von Bornstadt, D., Wei, Y., Balcioglu, A., DSelective ROCK 2 inhibition in focal cerebral ischemia. *Annals of Clinical and Translational Neurology,* 1(1), p. 2–14.

Leng, X. H. et al., 2004. Platelets of female mice are intrinsically more sensitive to agonists than are platelets of males. *Arterioscler Thromb Vasc Biol,* 24(2), pp. 376-381.

Lin, M. P. & Sanossian, N., 2015. Reperfusion therapy in the acute management of ischemic stroke. *Cardiol Clin,* Volume 33, pp. 99-109.

Lisabeth, L. & Bushnell, C., 2012. Stroke risk in women: The role of menopause and hormone therapy. *The Lancet Neurology,* 11(1), pp. 82-91.

Lisabeth, L. & Bushnell, C., 2012. Stroke risk in women: The role of menopause and hormone therapy. *The Lancet Neurology,* Volume 11, pp. 82-91.

Li, T. et al., 2014. Age and sex differences in vascular responsiveness in healthy and traumapatients: contribution of estrogen receptor-mediated Rho kinaseand PKC pathways. *Am J Physiol Heart Circ Physiol,* Volume 306, p. H1105–H1115.

Liu, P. Y., Death, A. K. & Handelsman, D. J., 2003. Androgens and cardiovascular disease. *Endocr Rev,* Volume 24, p. 313–340.

Liu, R. et al., 2005. 17beta-Estradiol attenuates blood-brain barrier disruption induced by cerebral ischemia-reperfusion injury in female rats. *Brain Res,* Volume 1060, pp. 55-61.

Lu, H. et al., 2017. Hemodynamic effects of intraoperative anesthetics administration in photothrombotic stroke model: A study using laser speckle imaging. *BMC Neurosci,* 18(10), pp. 1-8.

Lu, H. et al., 2014. Induction and imaging of photothrombotic stroke in conscious and freely moving rats. *Journal of Biomedical Optics,* 19(9), p. 0960134.

Madsen, T. E. et al., 2019. Temporal Trends of Sex Differences in Transient Ischemic Attack Incidence Within a Population. *J Stroke Cerebrovasc Dis,* 28(9), pp. 2468-2474.

Maggio, P., Salinet, A. S., Panerai, R. B. & Robinson, T. G., 2013. Does hypercapnia-induced impairment of cerebral autoregulation affect neurovascular coupling? A functional TCD study. *J Appl Physiol,* 115(4), pp. 491-497.

McCullough, L. D. et al., 2001. Postischemic estrogen reduces hypoperfusion and secondary ischemia after experimental stroke. *Stroke,* Volume 32, pp. 796-802.

McNeill, A. M. et al., 1999. Chronic estrogen treatment increases levels of endothelial nitric oxide synthase protein in rat cerebral microvessels. *Stroke,* Volume 30, pp. 2186-2190.

Mendelsohn, M. E. & Karas, R. H., 1999. The protective effects of estrogen on the cardiovascular system. *N Engl J Med,* Volume 340, pp. 1801-1811.

Miller, C. H., Rice, A. S., Garrett, K. & Stein, S. F., 2014. Gender, race and diet affect platelet function tests in normal subjects, contributing to a high rate of abnormal results. *Br J Haematol,* 165(6), pp. 842-853.

Ming, X. F. et al., 2002. Rho GTPase/Rho kinase negatively regulates endothelial nitric oxide synthase phosphorylation through the inhibition of protein kinase B/Akt in human endothelial cells. *Mol Cell Biol,* Volume 22, pp. 8467-8477.

Mishra, A. et al., 2016. Astrocytes mediate neurovascular signaling to capillary pericytes but not to arterioles. *Nature Neuroscience,* Volume 19, pp. 1619-1627.

Miyazaki-Akita, A. et al., 2007. 17beta-estradiol antagonizes the down-regulation of endothelial nitric-oxide synthase and GTP cyclohydrolase I by high glucose: relevance to postmenopausal diabetic cardiovascular disease. *J Pharmacol Exp Ther,* 320(2), pp. 591-598;.

Moshayedi, P. & Liebeskind, D. S., 2021. Chapter 28: Hemodynamics in acute stroke: Cerebral and cardiac complications. *Handbook of Clinical Neurology, Heart and Neurologic Disease,* Volume 177, pp. 295-317.

Moskowitz, M. A., Lo, E. H. & Iadecola, C., 2010. The science of stroke: mechanisms in search of treatments. *Neuron,* 67(2), pp. 181-198.

Nahirney, P. C., Reeson, P. & Brown, C. E., 2016. Ultrastructural analysis of blood-brain barrier breakdown in the peri-infarct zone in young adult and aged mice. *J Cereb Blood Flow Metab,* Volume 36, pp. 413-425.

Noma, K., Kihara, Y. & Higashi, Y., 2012. Striking crosstalk of ROCK signaling with endothelial function. 60(1), pp. 1-6.

Novella, S. et al., 2012. Vascular aging in women: Is estrogen the fountain of youth?. *Frontiers in Physiology,* Volume 3, pp. 1-8.

Nunes, K. P. & Webb, R. C., 2021. New insights into RhoA/Rho-kinase signaling: A key regulator of vascular contraction. *Small GTPases,* Volume 12, p. 458–469.

Nuno, D. W., Harrod, J. S. & Lamping, K. G., 2009. Sex-dependent differences in Rho activation contribute to contractile dysfunction in type 2 diabetic mice. *Am J Physiol Heart Circ Physiol*, 297(4), pp. H1469-1477.

Nuno, D. W., Korovkina, V. P., England, S. K. & Lamping, K. G., 2007. RhoA activation contributes to sex differences in vascular contractions. *Arterioscler Thromb Vasc Biol,* 27(9), pp. 1934-1940.

Ohtsuki, S. et al., 2005. Dominant expression of androgen receptors and their functional regulation of organic anion transporter 3 in rat brain capillary endothelial cells; Comparison of gene expression between the blood-brain and -retinal barriers.. *J Cell Physiol,* Volume 204, pp. 896-900.

Orshal, J. M. & Khalil, R. A., 2004. Gender, sex hormones, and vascular tone. *Am J Physiol Regul Integr Comp Physiol,* Volume 286, pp. R233-249.

Otahbachi, M. et al., 2010. Gender differences in platelet aggregation in healthy individuals. *J Thromb Thrombolysis,* 30(2), pp. 184-191.

Park, L. et al., 2005. NADPH-oxidase-derived reactive oxygen species mediate the cerebrovascular dysfunction induced by the amyloid beta peptide. *J Neurosci,* Volume 25, pp. 1769-1777.

Penotti, M. et al., 2001. Effects of androgen supplementation of hormone replacement therapy on the vascular reactivity of cerebral arteries. *Fertility and sterility,* 76(2), pp. 235-240.

Persky, R. W., Turtzo, L. C. & McCullough, L. D., 2010. Stroke in women: disparities and outcomes. *Curr Cardiol Rep,* Volume 12, pp. 6-13.

Peters, A. et al., 2004. The selfish brain: Competition for energy resources. *Neurosci Biobehav Rev,* 28(2), pp. 143-180.

Prabhakaran, S., Ruff, I. & Bernstein, R. A., 2015. Acute stroke intervention: a systematic review. *JAMA,* Volume 313, pp. 1451-1462.

Pradeep, H., Diya, J. B., Shashikumar, S. & Rajanikant, G. K., 2012. Oxidative stress--assassin behind the ischemic stroke. *Folia Neuropathol,* Volume 50, pp. 219-230.

Profaci, C. P., Munji, R. N., Pulido, R. S. & Daneman, R., 2020. The blood-brain barrier in health and disease: Important unanswered questions. *J Exp Med,* Volume 217, pp. 1-16.

Rakymzhan, A., Li, Y., Tang, P. & Wang, R. k., 2021. Differences in cerebral blood vasculature and flow in awake and anesthetized mouse cortex revealed by quantitative optical coherence tomography angiography. *Journal of Neuroscience Methods,* 353(109094), pp. 1-8.

Rankinen, T. et al., 2008. A major haplotype block at the rho-associated kinase 2 locus is associated with a lower risk of hypertension in a recessive manner: The HYPGENE study. *Hypertens Res,* Volume 31, p. 1651–1657.

Rashid, P. A., Whitehurst, A., Lawson, N. & Bath, P., 2003. Plasma nitric oxide (nitrate/nitrite) levels in acute stroke and their relationship with severity and outcome. *J Stroke Cerebrovasc Dis,* Volume 12, pp. 82-87.

Razmara, A. et al., 2008. Mitochondrial effects of estrogen are mediated by estrogen receptor alpha in brain endothelial cells. *J Pharmacol Exp Ther,* Volume 325, pp. 782-790.

Reckelhoff, J. F., 2001. Gender differences in the regulation of blood pressure. *Hypertension,* Volume 37, pp. 1199-1208.

Reckelhoff, J. F., 2007. Polycystic ovary syndrome: androgens and hypertension. *Hypertension,* Volume 49, p. 1220–1221.

Riento, K. & Ridley, A. J., 2003. ROCKs: Multifunctional kinases in cell behaviour. *Nature Reviews Molecular Cell Biology,* Volume 4, p. 446–456.

Rikitake, Y. et al., 2005. Inhibition of Rho kinase (ROCK) leads to increased cerebral blood flow and stroke protection. *Stroke,* Volume 36, pp. 2251-2257.

Ritzel, R. M., Capozzi, L. A. & McCullough, L. D., 2013. Sex, Stroke, and Inflammation: The potential for Estrogen-mediated immunoprotection in stroke. *Horm Behav,* 63(2), p. 238–253.

Rivera, P., Ocaranza, M. P., Lavandero, S. & Jalil, J. E., 2007. Rho kinase activation and gene expression related to vascular remodeling in normotensive rats with high angiotensin I converting enzyme levels. *Hypertension,* Volume 50, pp. 792-798.

Rodrigo, R. et al., 2013. Oxidative stress and pathophysiology of ischemic stroke: novel therapeutic opportunities. *CNS Neurol Disord Drug Targets,* Volume 12, pp. 698-7.

Rosenblum, W. I., el-Sabban, F., Allen, A. D. & Nelson, G. H., 1985. Effects of estradiol on platelet aggregation in cerebral microvessels of mice. *Stroke,* 16(6), p. 980–984.

Rosenblum, W. I. et al., 1987. Effects in mice of testosterone and dihydrotestosterone on platelet aggregation in injured arterioles and ex vivo. *Thrombosis Research,* 45(6), pp. 719-728.

Salinet, A. S., Robinson, T. G. & Panerai, R. B., 2013. Cerebral blood flow response to neural activation after acute ischemic stroke: a failure of myogenic regulation?. *J Neurol,* 260(10), pp. 2588-95.

Samdani, A. F., Dawson, T. M. & Dawson , V. L., 1997. Nitric oxide synthase in models of focal ischemia. *Stroke,* Volume 28, pp. 1283-1288.

Sandberg, K. & Ji, H., 2012. Sex differences in primary hypertension. *Biol Sex Differ,* 3(7), pp. 1-21.

Satoh, S. et al., 2010. Amelioration of endothelial damage/dysfunction is a possible mechanism for the neuroprotective effects of Rho-kinase inhibitors against ischemic brain damage. *Brain Res Bull,* 81(1), pp. 191-195.

Sawada, N. & Liao, J. K., 2009. Targeting eNOS and beyond: emerging heterogeneity of the role of endothelial Rho proteins in stroke protection.. *Expert Rev Neurother,* Volume 9, pp. 1171-1186.

Schubert, P. et al., 2016. RhoA/ROCK signaling contributes to sex differences in the activation of human platelets. *Thromb Res,* Volume 139, pp. 50-55.

Schubert, P. et al., 2016. RhoA/ROCK signaling contributes to sex differences in the activation of human platelets. *Thromb Res,* Volume 139, pp. 50-55.

Selvaraj, U. M. et al., 2018. Selective Nonnuclear Estrogen Receptor Activation Decreases Stroke Severity and Promotes Functional Recovery in Female Mice. *Endocrinology,* Volume 159, pp. 3848-3859.

Shi, H. & Liu, K. J., 2007. Cerebral tissue oxygenation and oxidative brain injury during ischemia and reperfusion. *Front Biosci,* Volume 12, pp. 1318-1328.

Shimizu, T. & Liao, J. K., 2014. Rho kinases and cardiac remodeling. *Circulation,* 80(7), pp. 1491-1498.

Shin, H. K. et al., 2007. Rho-kinase inhibition acutely augments blood flow in focal cerebral ischemia via endothelial mechanisms. *J Cereb Blood Flow Metab,* Volume 27, pp. 998-1009.

Shin, J. A., Yoon, J. C., Kim, M. & Park, E. M., 2016. Activation of classical estrogen receptor subtypes reduces tight junction disruption of brain endothelial cells under ischemia/reperfusion injury. *Free Radic Biol Med,* Volume 92, pp. 78-89.

Siddiqui, M. R. et al., 2011. Caveolin-1-eNOS signaling promotes p190RhoGAP-A nitration and endothelial permeability. *J Cell Biol,* Volume 193, pp. 841-850.

Silva, G. S. et al., 2010. Gender differences in outcomes after ischemic stroke: role of ischemic lesion volume and intracranial large-artery occlusion. *Cerebrovasc Dis,* 30(5), pp. 470-475.

Simoncini, T. et al., 2000. Interaction of oestrogen receptor with the regulatory subunit of phosphatidylinositol-3-OH kinase. *Nature,* 407(6803), pp. 538-541.

Sladojevic, N. et al., 2017. Decreased thromboembolic stroke but not atherosclerosis or vascular remodelling in mice with ROCK2-deficient platelets. *Cardiovasc Res,* 113(11), pp. 1307-1317.

Soliman, H. et al., 2012. Diabetes-induced increased oxidative stress in cardiomyocytes is sustained by a positive feedback loop involving Rho kinase and PKCβ2. *The American Journal of Physiology-Heart and Circulatory Physiology,* 303(8), pp. H989-H1000.

Sopko, N. A., Hannan, J. L. & Bivalacqua, T. J., 2014. Understanding and targeting the Rho kinase pathway in erectile dysfunction. *Nat Rev Urol,* 11(11), p. 622–628.

Statistics Canada, 2017. Table 102–0561 – Leading causes of death, total population, by age group and sex, Canada.. *CANSIM (death database).*

Sugimoto, M. et al., 2007. Rho-kinase phosphorylates eNOS at threonine 495 in endothelial cells. *Biochem Biophys Res Commun,* Volume 361, pp. 462-467.

Tajima, Y. et al., 2014. Reproducibility of measuring cerebral blood flow by laser-Doppler flowmetry in mice. *Front Biosci (Elite Ed),* 6(1), pp. 62-68.

Takemoto, M. et al., 2002. Rho-Kinase Mediates Hypoxia-Induced Downregulation of Endothelial Nitric Oxide Synthase. *Circulation,* 106(1), p. 57–62.

Takeuchi, K. et al., 2013. AMP-dependent kinase inhibits oxidative stress-induced caveolin-1 phosphorylation and endocytosis by suppressing the dissociation between c-Abl and Prdx1 proteins in endothelial cells. *J Biol Chem,* Volume 288, pp. 20581-20591.

Tang, F. C. et al., 2017. Simvastatin attenuated rat thoracic aorta remodeling by decreasing ROCK2mediated CyPA secretion and CD147ERK1/2cyclin pathway. *Mol Med Rep,* Volume 16, pp. 8123-8129.

Toda, N., 2012. Age-related changes in endothelial function and blood flow regulation. *Pharmacol Ther,* Volume 133, pp. 159-176.

Toda, N., Ayajiki, K. & Okamura, T., 2009. Cerebral blood flow regulation by nitric oxide in neurological disorders. *Can J Physiol Pharmacol,* Volume 87, pp. 581-594.

Tuma, P. & Hubbard, A. L., 2003. Transcytosis: crossing cellular barriers. *Physiol Rev,* Volume 83, pp. 871-932.

Turtzo, L. C. & McCullough, L. D., 2008. Sex differences in stroke. *Cerebrovascular Diseases,* Volume 26, pp. 462-474.

Turtzo, L. C. & McCullough, L. D., 2010. Sex-specific responses to stroke. *Future Neurol,* Volume 5, pp. 47-59.

Tymianski, M., 2011. Emerging mechanisms of disrupted cellular signaling in brain ischemia. *Nature Neuroscience,* 14(11), pp. 1369-73.

Vaughan, C. J. & Delanty, N., 1999. Neuroprotective properties of statins in cerebral ischemia and stroke. *Stroke,* Volume 30, pp. 1969-1973.

Wang, F. et al., 2018. Dysfunction of Cerebrovascular Endothelial Cells: Prelude to Vascular Dementia. *Front Aging Neurosci,* Volume 10, pp. 1-23.

Wang, Y. et al., 2019. Sex difference in the incidence of stroke and its corresponding influence factors: results from a follow-up 8.4 years of rural China hypertensive prospective cohort study. *Lipids Health Dis, 18, 72.,* Volume 18, p. 72.

Wang, Y. et al., 2009. ROCK isoform regulation of myosin phosphatase and contractility in vascular smooth muscle cells. *Circulation,* Volume 104, pp. 531-540.

Wassertheil-Smoller, S. et al., 2003. Effect of estrogen plus progestin on stroke in postmenopausal women: The Women's Health Initiative: A randomized trial. *JAMA,* Volume 289, pp. 2673-2684.

Willie, C. K., Tzeng, Y. C., Fisher, J. A. & Ainslie, P. N., 2014. Integrative regulation of human brain blood flow. *The Journal of Physiology,* 592(5), pp. 841-859.

Xiao, H. et al., 2018. Pretreatment with 17beta-Estradiol Attenuates Cerebral Ischemia-Induced Blood-Brain Barrier Disruption in Aged Rats: Involvement of Antioxidant Signaling. *Neuroendocrinology,* Volume 106, pp. 20-29.

Xu, C. et al., 2016. Astragaloside IV improves the isoproterenol-induced vascular dysfunction via attenuating eNOS uncoupling-mediated oxidative stress and inhibiting ROS-NF-kappaB pathways. *Int Immunopharmacol,* Volume 33, pp. 119-127.

Xue, B. et al., 2009. Sex differences and central protective effect of 17betaestradiol in the development of aldosterone/NaCl-induced hypertension. *Am J Physiol Heart Circ Physiol,* Volume 296, p. H1577–H1585.

Xue, B. et al., 2014. Estrogen regulation of the brain renin-angiotensin system in protection against angiotensin II-induced sensitization of hypertension. *Am J Physiol Heart Circ Physiol,* Volume 307, p. H191–H198.

Yamada, M. et al., 2000. Endothelial nitric oxide synthase-dependent cerebral blood flow augmentation by L-arginine after chronic statin treatment. *Journal of Cerebral Blood Flow and Metabolism,* 20(4), pp. 709-17.

Yang, S. H., Shi, J., Day, A. L. & Simpkins, J. W., 2000. Estradiol exerts neuroprotective effects when administered after ischemic insult. *Stroke,* Volume 31, pp. 745-750.

Yang, S. et al., 2019. Longitudinal in vivo intrinsic optical imaging of cortical blood perfusion and tissue damage in focal photothrombosis stroke model. *J Cereb Blood Flow Metab,* Volume 39, pp. 1381-1393.

Yao, L. et al., 2010. The role of RhoA/Rho kinase pathway in endothelial dysfunction. *J Cardiovasc Dis Res,* Volume 1, pp. 165-170.

Yu, Q. J., Tao, H., Wang, X. & Li, M. C., 2015. Targeting brain microvascular endothelial cells: A therapeutic approach to neuroprotection against stroke. *Neural Regeneration Research,* 10(11), pp. 1882-1891.

Zhang, Z. G. et al., 2002. Correlation of VEGF and angiopoietin expression with disruption of blood-brain barrier and angiogenesis after focal cerebral ischemia. *J Cereb Blood Flow Metab,* Volume 22, pp. 379-392.

Zhao, Y., Vanhoutte, P. M. & Leung, S. W. S., 2015. Vascular nitric oxide: Beyond eNOS. *Journal of Pharmacological Sciences,* Volume 129, pp. 83-94.

Zhu, J., Song, W., Li, L. & Fan, X., 2016. Endothelial nitric oxide synthase: a potential therapeutic target for cerebrovascular diseases. *Molecular Brain,* Volume 9, pp. 1-8.

Zhu, Y. et al., 2003. Low density lipoprotein induces eNOS translocation to membrane caveolae: the role of RhoA activation and stress fiber formation. *Biochim Biophys Acta,*, Volume 1635, pp. 117-126.

Zwierzina, W. D., Kunz, F., Kogelnig, R. & Herold, M., 1987. Sex-related differences in platelet aggregation in native whole blood. *Thrombosis Research,* 48(2), pp. 161-171.